Preparation and Characterization of Ce-Doped Lead Lanthanum Titanate (PLT) Thin Films

By

BANASHREE ROY

MATERIALS SCIENCE PROGREAMME

INDIAN INSTITUTE OF TECHNOLOGY KANPUR

July 1999

Preparation and Characterization of Ce-Doped Lead Lanthanum Titanate (PLT) Thin Films

A Thesis Submitted in Partial Fulfillment of the
Requirements for the Degree of Master of Technology

By
Banashree Roy

MATERIALS SCIENCE PROGREAMME
INDIAN INSTITUTE OF TECHNOLOGY, KANPUR
JULY, 1999

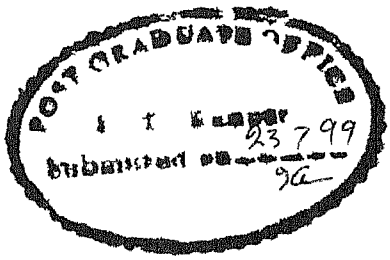

Certificate

It is certified that the work contained in this thesis entitled ***"Preparation and Characterization of Ce-Doped Lead Lanthanum Titanate (PLT) Thin Films"*** by Banashree Roy has been cried out under our supervision and that this thesis has not been submitted elsewhere for any degree

Y N Mohapatra
July 1999

D C Agrawal
27 July 1999

Dedicated to My Parents

(Baba o Ma ka)

Acknowledgement

I joined M Tech in Materials Science with ceramic engineering background Ideally one would expect a thesis in ceramic science as natural choice It was sheer chance that I got an opportunity to enter the field of electroceramics under Prof D C Agrawal who also taught me two ceramic based courses Initially I was nervous But slowly with the encouragement and excellent guidance of Dr Agrawal the initial nervousness turned in to an exiting interest For this emotional transformation for which Prof Agrawal was the sole force I have absolutely no words to express my gratitude I am able to finish my thesis only due to his guidance intellectual support and creative criticism

I express my deep sense of gratitude to Dr Y N Mohapatra for his deep insight and guidance for my thesis work With each and every interaction I learnt some concepts in ferroelectrics not known to me earlier

I am grateful to Subhasish da whom I met at the time of starting my thesis He is a treasure of knowledge and experience in ferroelectric ceramics He practically introduced me in to the research world of ferroelectric ceramic thin films by virtually leading me by hand He tought me every essential step from samples preparation to electrical measurements He answered lots of my doubts sometimes childish with great patience treating me just like his younger sister

I am especially thankful to Mishraji Many times he helped me with his strong technical experience and vast knowledge in electroceramics Many a times his fatherly wise suggestions helped me to overcome my frustrated situations

I want to thank my ex laboratory mate and my senior Soumen for providing the programme for calculating the lattice parameters of the crystals

I am thankful to my hostel mates Madhu Jayashree Arpita Pragya Chanda etc for their loving and warm company I want to express my hearty gratitude especially to my bosom friend Shampa who made my memory of stay in IITK a pleasant and cherishable one

Thanks are due to my labmates (ex and present) Atanu da Bhoumik Pankaj Rashmi Satosh Sarika Amit and Dube for their cooperative and helping attitude and for creating a pleasant and homely atmosphere in the Laboratory

I am grateful to all ACMS laboratory and staff members specially Bishwanathji Umashankarji and Mr Jain for their hearty help which made my thesis work easy

Finally I will never forget the moral support I get from my family My parents are my constant source of inspiration and encouragement Their love faith and hope will always show me the way for success in life

Abstract

Lead lanthanum titanate (PLT) has very attractive pyroelectric properties But its ferroelectric properties are poor Ce is known to enhance the ferroelectric properties of lead zirconium titanate (PZT) thin films We have therefore studied the effect of Ce on the ferroelectric properties of PLT thin films Ce doped PLT thin films of four different compositions ($PL_{15}T$ $PL_{12}C_{03}T$ $PL_{10}C_{05}T$ and $PL_{08}T_{07}T$) have been prepared by sol gel method on polycrystalline Pt and sapphire substrates by means of the spin coating technique The phases of the films were studied by X ray diffraction method It is found that with increasing Ce content the c axis orientation of the films increases for both the substrates Highest degree of c axis orientation is obtained in the $PL_{10}C_{05}T$ film Above 5 at % Ce c axis orientation of the films decreases Time temperature-transformation (TTT) study of $PL_{15}T$ films show that PLT films crystallize at much lower temperature than PZT films and the perovskite formation is easier The dielectric and ferroelectric properties of the films are characterized P_r and P_s (remnant and saturation polarization respectively) of the films increase with Ce content and comes to the highest value for the $PL_{10}C_{05}T$ film ($P_s \sim 54\ 00$ $P_r \sim 34\ 00$) The dielectric constant vary from 990 to 1415 for Ce content of the films from 0 at % to 7 at % respectively with $PL_{10}C_{05}T$ film having the highest value of 1520 Values of dielectric losses are also consistent with that of ferroelectric and dielectric constant values C axis orientation of the films supports this particular trend of characteristics In conclusion it is found that Ce doping in PLT thin films enhances the ferroelectic and dielectric properties of the films and PLT thin film with 5 at % Ce has the best ferroelectric properties

Contents

List of Figures

List of Tables

Chapter 1

Introduction

1 1 Point groups and ferroelectricity

Crystals depending on their geometry are classified into seven systems and these seven systems are again divided into 32 point groups with respect to their symmetry around a point (Fig 1 1) 11 of these point groups possess a centre of symmetry and so are non polar in nature Other 21 are non centro symmetric Among these 21 20 exhibit piezoelectricity (stress/strain dependant polarization) 10 of these 20 show spontaneous polarization which is in general temperature dependant It is called pyroelectric effect and these crystals are called pyroelectric crystals A limited numbers of pyroelectric materials have the additional property that the direction of the spontaneous polarization can be changed by an applied electric field This special group of materials is called ferroelectric materials This reversible polarization results in the existence of a hysteresis loop when the field applied is plotted against the resulting polarization A typical loop is shown in the Figurel 2 The observation of hysteresis loop is done basically using the original or the modified Sawyer Tower circuit [1] At low and at very high fields the ferroelectric materials behave like an ordinary dielectric (usually with a high dielectric constant) but in the medium fields (~ E_c) region polarization reversal occurs giving a large dielectric non linearity The area within the loop is a measure of the energy required to twice reverse the polarization

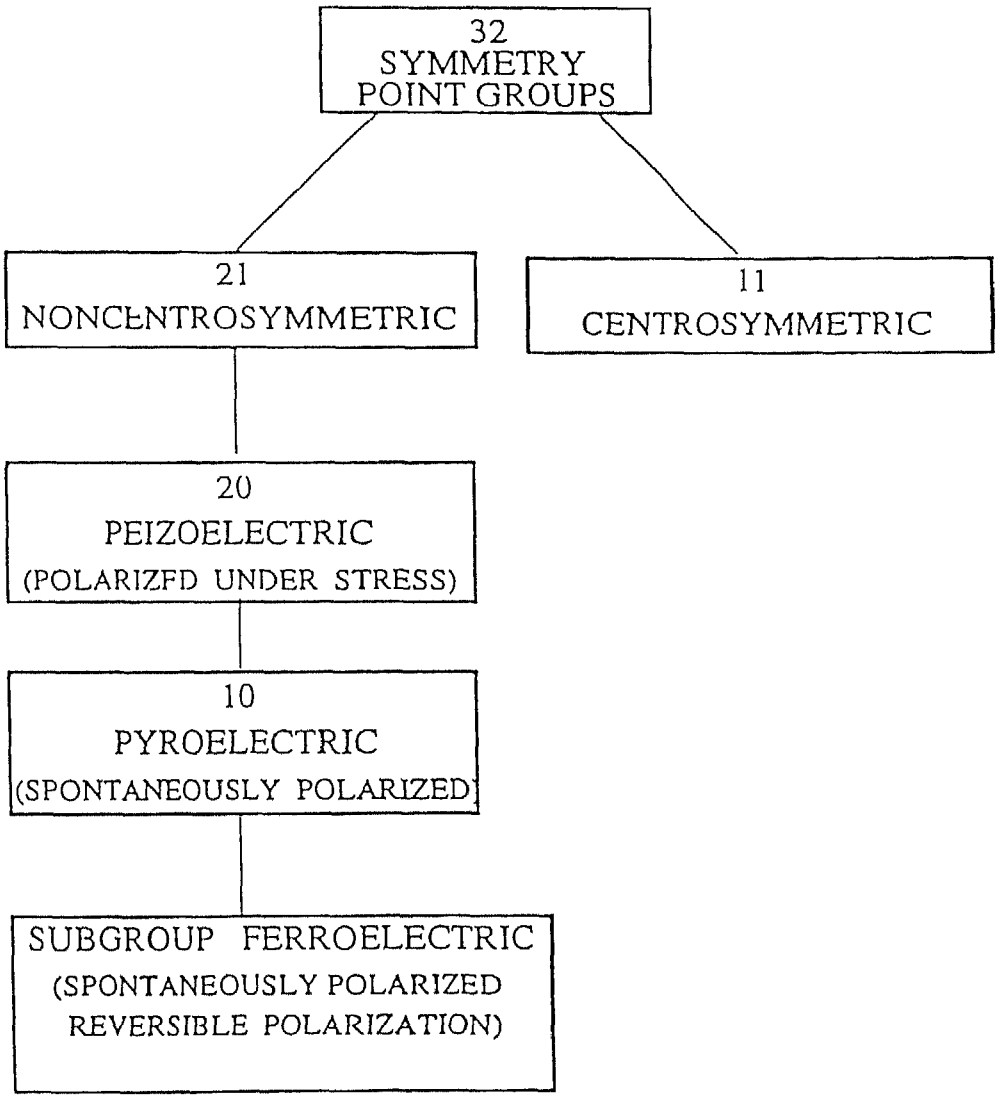

Fig 1 1 Interrelationship of the piezoelectrics and subgroups on the basis of internal crystal symmetry [2]

In the figure of hysteresis loop P_s is the saturation polarization which can be obtained by extrapolating the saturation value of the electric polarization to the zero field (E) P_r is the remnant polarization which is the value of polarization at zero field and E_c

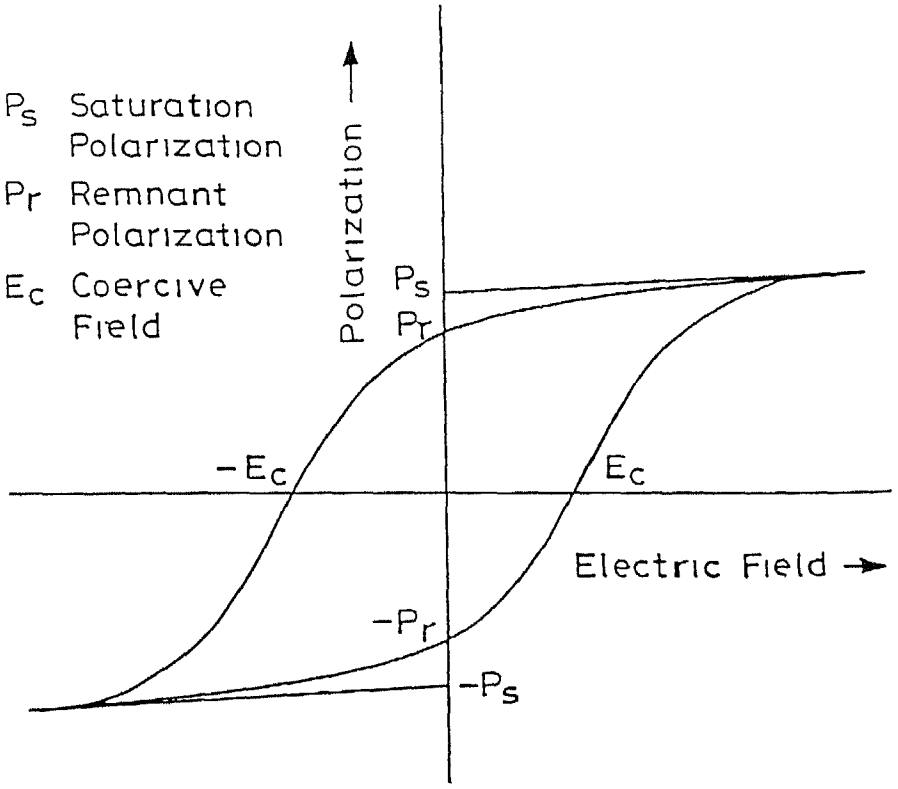

Fig 1 2 Typical hysteresis loop of ferroelectric ceramics

coercive field is the value of the field at which polarization reversal occurs giving a large dielectric non linearity

1 2 Ferroelectric and Pyroelectric Ceramics

Although initially most theoretical works and experimental study on the fundamental ferroelectric properties and the commercial uses were carried out on large single crystals (due to the fact that they have less imperfections and surface defects) use of polycrystalline ceramic materials is of practical importance because of

1 the possibility of preparing a wide range of compositions

2 the corresponding ability to adjust their properties for different applications

Ferroelectric polycrystalline ceramics are much easier to prepare than the single crystals and in many cases they show good ferroelectric and pyroelectric properties comparable to those of the single crystals

1 2 1 Application of ferroelectric and pyroelectric materials

Several phenomena in ferroelectric materials such as pyroelectricity and piezoelectricity and polarization hysteresis may be exploited to fabricate a number of useful devices These are as follows

The main uses of the ferroelectric thin films are as capacitative elements and as memory devices Memory elements are of two types

1 Dynamic random memory (DRAM) for which the thin films should have high dielectric constant low loss factor and low leakage current density

2 Non volatile random accesses memory (NVRAM) for which low coercive field (E_c) high remnant polarization (P_r) and very small switching time for polarization are necessary

One of the most important uses of the pyroelectric materials is as IR detector In a pyroelectric material there is a change of spontaneous polarization due to change of temperature This lead to the appearance of a pyroelectric current which is proportional to the rate of change of temperature This change of temperature can be brought about by chopped IR radiation and the current produce can be used to detect and to measure the IR radiation The pyroelectric current (I_P) is related with the change of temperature (T) with time as follows

$$I_P = \rho A T \qquad (1\ 1)$$

Where ρ = pyroelectric co efficient and

A = area of the pyroelectric detector element on which the radiation falls

This kind of detector can detect the existence of moving elements or humans The moving body emits radiation which is detected by detector

This types of IR detectors are also used in radiometry

Pyroelectric detectors are also used in pollutant control The IR radiation is passed through tube containing the gas with pollutant and radiation is passed through an optical

filter corresponding to a frequency at which the pollutant absorbs radiation to a greater extent than any other constituents of the gas The presence of pollutant can be detected by comparing the result with the result obtained by using other filter of different wavelength to which the gas is transparent

It is used for preparing the intruder alarm in thermal imaging etc In an IR FET detector a pyroelectric film is deposited on top of the gate oxide layer which act as an integrated sensor [3]

In principal ferroelectrics are also piezoelectric A potential application for piezoelectric materials is micropositioning and actuation for micromotors These materials have a number of other uses also Among these surface acoustic wave device (SAW) in particular very important

1 2 2 Changes of Properties by Doping

One of the very significant advantages of the ceramic compounds is that their properties can be modified by addition of foreign ions substituting part of host atoms This technique is known as doping Dopants are of two types donor dopants and acceptor dopants The acceptor dopants have a lower valance than that of the substituted atoms and oxygen vacancies help to compensate this charge imbalance The donor dopants have higher charge than that of the replaced ions and this charge imbalance is compensated by cation vacancies Table 1 1 shows the common dopants in perovskite ceramics
The effects of the dopants are

1 Donor dopant replaces either A site or B site ions and produces p type ceramics and so the resistivity increases Generally on introducing the donor dopants A site vacancies are created Donor dopants enhance domain reorientation and donor doped ferroelectric ceramics are characterized by square hysteresis loops low coersivity high remnant polarization high dielectric constants, maximum coupling factors high dielectric loss reduced aging etc

2 Acceptors create negative charge which are balanced by oxygen vacancies But generally they have limited orientation in the lattice because of which he domain reorientation is limited and ceramics with acceptor additives show poorly developed hysteresis loops low dielectric constant and low dielectric loss high aging rate etc

3 Isovalent additives have the same valance as the substituted ions The solubility of these additives is high and on doping the ferroelectrics show low dielectric loss high aging rate etc

Table 1 1 Common aliovalent substituents

Detail of the dopants	Examples
A site donors	La^{+3} Bi^{+3} Nd^{+3}
B site donors	Nb^{+5} Ta^{+5} Sb^{+5}
A site acceptors	K^{+} Rb^{+}
B site acceptors	Co^{+3+} Fe^{+3} Sc^{+3} Ga^{+3} La^{+3} Cr^{+3} Mn^{+3} Mn^{+} Cu^{+2}

4 Multiple valance dopants act both as donar and acceptor So the properties of these ceramics are a mixture of donar and acceptor doped ceramics

1 3 The Lead Titanate ($PbTiO_3$) Based Ceramics

Among the ceramic ferroelectric compounds lead titanate (PT) based ceramics are important class of materials which find wide applications in piezoelectric and pyroelectric devices

Lead titanate (PT) has an ABO_3 type of perovskite structure The O atoms are at the face centered position A sites i e corners of the cell are occupied by the Pb^{+2} ions and B sites i e body centered position is occupied by the Ti^{+4} ions (Fig 1 3)

Ferroelectric nonferroelectric transition is accompanied by a phase change In case of the ferroelectric perovskite ceramics the temperature at which phase changes from cubic to tetragonal or rhombohedral is called the Curie point Sometimes the approaching transition is signaled by a diverging dielectric response or permitivity (ε) which close to

transition temperature (T_c) varies with temperature in an approximate Curie Weiss manner

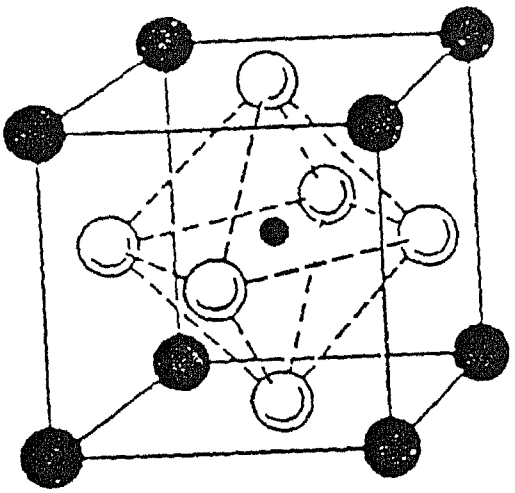

Fig 1 3 Structure of an ABO_3 perovskite crystal

$$\varepsilon = C/(T\ T_0) \qquad (1\ 2)$$

where T_0 = Curie Weiss temperature which is equal to Curie temperature (T_c) only for a continuous transition

Above Curie temperature the material is in paraelectric phase When the ferroelectric crystal is cooled from a paraelectric phase to a ferroelectric phase in the absence of applied fields depolarized crystal assumes a high energy on polarization

$$W_E = 1/2\int D\ E\ dV \qquad (1\ 3)$$

where D = Electric displacement

E= Field

and V= Volume of the crystal

To minimize this energy the crystal brakes into domains The polarization within a domain is uniform but the polar orientation of the different domains are not similar Without domain formation the energy of the crystal is much higher than the energy associated with ferroelectric ordering so that ferroelectricity can t exist But when a sufficiently high electric field is applied externally the domains tend to align along the field direction and the crystal obtains a net polarization

1 4 Ferroelectric Thin Films

The pyroelectric and ferroelectric ceramics are currently used mostly in the form of the bulk ceramics However using in thin film form offers number of advantage like

1 Crystallization and sintering of the thin films usually occur at hundreds of degrees lower than for bulk These lower temperatures are compatible with semi conductor processing temperature

2 Due to very small thickness the operating voltage can be reduced to few volts which are compatible with electronic circuit drive voltage

3 High charge storage density in small area leads to miniaturization of the devices

4 Epitaxial growth is relatively easier in thin film than the growth of single crystal in bulk

1 5 Preparation of ferroelectric thin films-the Sol-Gel Method

Different methods have been used for the preparation of the PLT thin films such as rf magnetron sputtering [4 8] chemical vapour deposition (CVD)[9] sol gel [10-12] pulse laser deposition (PLD) [13] etc depending on the application

Among the above mentioned techniques the sol gel method has the following advantages over the others

1 Homogeneity at the molecular level
2 Low preparation temperature saves energy
3 High deposition rate

4 Easy introduction of the dopants

5 Deposition under different ambient condition is possible

But sol gel process has some disadvantages also

1 Large shrinkage during processing and formation of cracks

2 Residual fine pores

3 Long processing time

4 Health hazards from organic solvents

Sol Gel method has been used for the preparation of films in this work

A sol is defined as a suspension of submicron particles in a liquid Sols can be of two types In one preparation is done by precipitation of particles in suspension such as in the preparation of SiO_2 sol

$$Na_2SiO_3 + 2HCl \rightarrow SiO_2 + 2NaCl + H_2O$$

A sol can also be prepared by starting with metal alkoxides

In this method a metal alkoxide such as $Si(OC_2H_5)$ (tetraethyl orthosilicate TEOS) and water are mixed together in a common solvent which is usually an alcohol A small amount of an acid or a base is added as a catalyst Two types of reactions proceed simultaneously

(i) hydrolysis

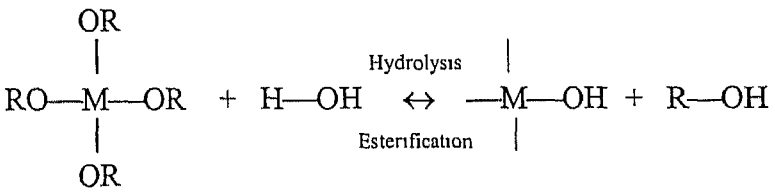

(1 4)

(ii) condensation

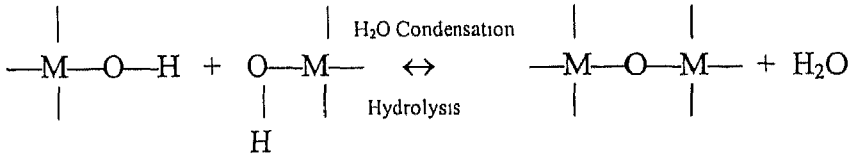

(1 5)

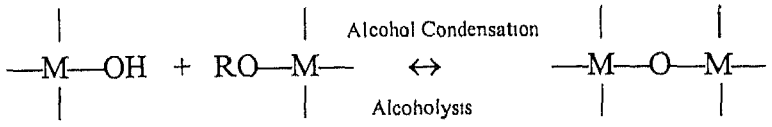

(1 6)

Due to these reactions oligomers containing a few metal atoms form These oligomers suspended in the liquid constitute the sol

1 5 1 Mechanism of Hydrolysis

1 5 1 1 Acid –Catalyzed Hydrolysis

Different workers have proposed different mechanisms for the acid catalyzed hydrolysis [14 20] Some of them proposed a possible acid catalyzed hydrolysis mechanism as follow (1 7) In this mechanism lone pair electron of Oxygen of water attack the $Si^{+\delta}$ without inversion of the silicon tetrahedron Klemperer et al [21] showed same type of mechanism

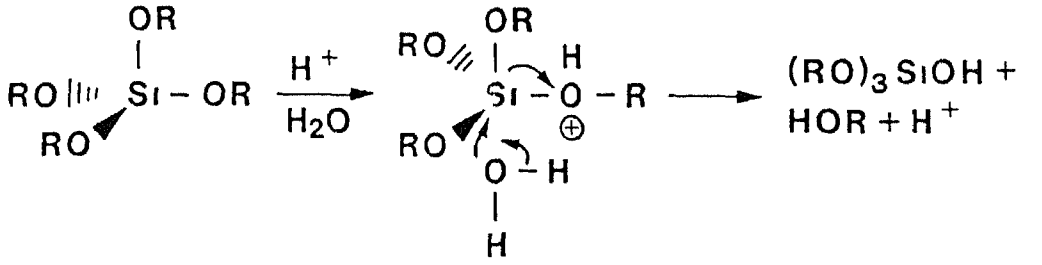

(1 7)

In acid catalyzed reaction with the substitution of 1st —OR group with —OH group rate of hydrolysis decreases because R has much more electron donating capacity than H For this cause on acid catalyzed hydrolysis two dimensional chain like structure formed

1 5 1 2 Base-Catalyzed Hydrolysis

Iler [22] and Keefer [14] proposed an S_N2 Si mechanism (1 8) But it is affected by steric and inductive factors

Pohl and Osterholtz [15] described S_N2 * Si or S_N2^* Si mechanism with a stable 5 coordinate intermediate state (1 9)

In this mechanism as —OR group has more electron donating capacity than —OH group the Si of the tetrahedral has less positive charge density to be attracted by OH^- group in the 1st hydrolysis But with the incorporation of —OH group it become more

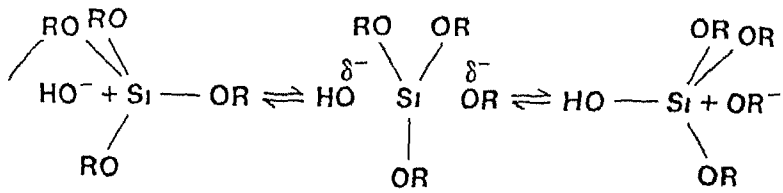

(1 8)

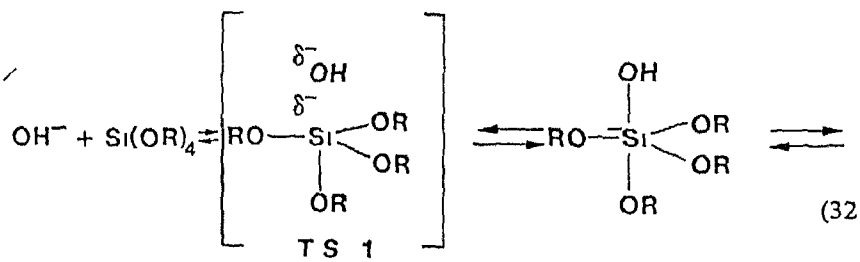

(1 9)

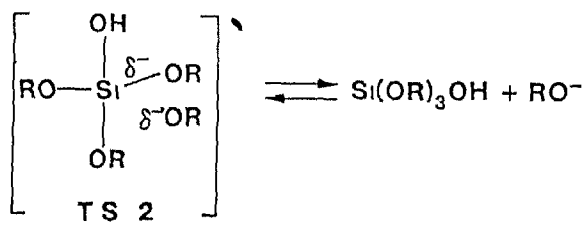

easier and 1st step of hydrolysis actually enhances the next step For this cause on base catalyzed hydrolysis 3 dimentional branched network is formed

1 5 2 Condensation and Gelation

Gelation of the sol is the next step Under suitable conditions sol is transformed to a gel which can be defined as a rigid continuous porous mass network produced through destabilization precipitation or supersaturation Both hydrolysis and condensation occur simultaneously The relative rate of the two reactions reaction depends on the conditions of the experiment i e catalyst type solvent temperature pressure water and alkoxide ratio inductive effect presence of steric group in molecule etc Among these factors water and alkoxide ratio is the most important Since water is the by product of condensation action addition of more water suppresses the reaction to words the left according to the La

Chatelier s principle So more hydrolysis will occur Fig 1 4 [23] shows the variation of gelation time with increasing amount of water in silicon ethoxide gel formation

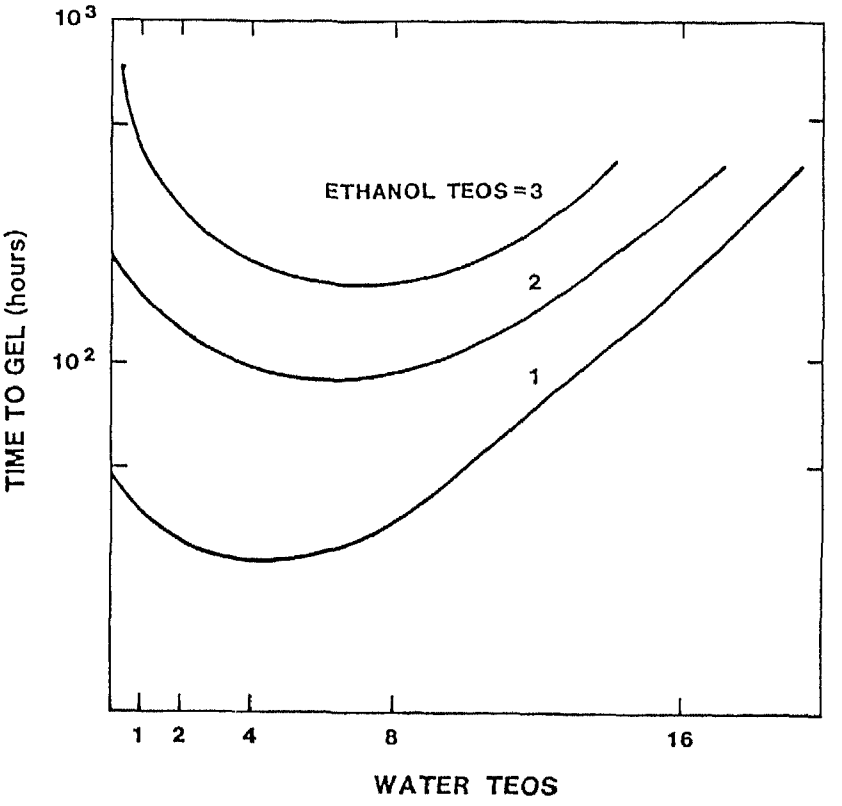

Fig 1 4 Gel time vs water TEOS ratio [23]

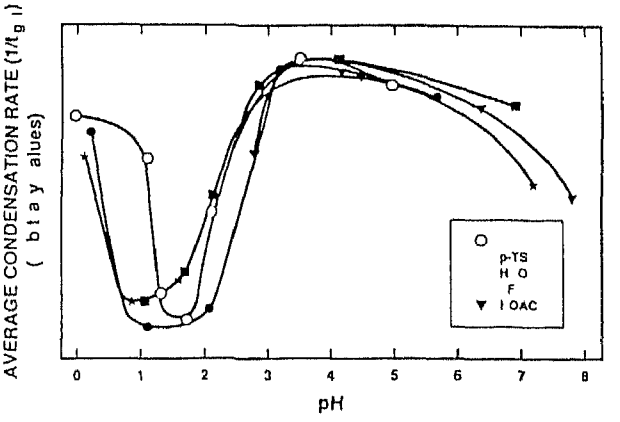

Fig 1 5 Average condensation rate for TEOS hydrolyzed with solution of various acids [24]

Fig 1 5 [24] shows the effect of pH on the average condensation rate ($1/t_{gel}$) for the TEOS

Table 1 2 shows the variation of gelation time for those hydrolyzed in different solvents

Table 1 2 Gel time for TMOS hydrolyzed in different solvents [25]

Solvent	t_{gel}(min)
Methanol	8
Formamide	6
Dimethyl Formamide	28
Acetonitrile	23
Dioxane	41

Rheological measurements characterize the bulk properties of the sol Rheological properties are highly dependant on the concentration of sol molecular weight and shear rate For organic polymers it is shown that viscosity (η) is related to number average molecular weight (M_n) according [26] to the following formula

$$[\eta] = KM_n^{\alpha} \qquad (1\ 10)$$

where K= Constant depends on polymer

and α depends on polymer structure

Numbers of scientists [26 28] worked on the viscosity of the sol gel transition Sakka et al showed [27] that the gel point is defined as the time at which the viscosity is observed to increase abruptly (Fig 1 6)

By controlling viscosity of sol gel transition different kinds of shapes can be given to sol At about 1 cP viscosity partially hydrolyzed sol can be coated on the substrates and form films About 10 cp when the sol turns into somewhere a sticky mass fiber can be drown from it

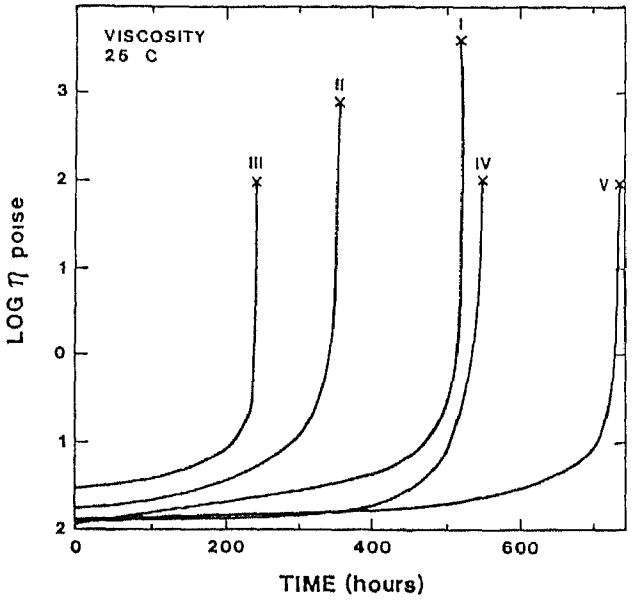

Fig 1 6 Change of viscosity for hydrolyzed TEOS with time [27]

1 6 Literature Review on La Doped PT Thin Film

Since 1970 s the scientists have been working on the properties and characteristics of $PbTiO_3$ thin films They have shown that $PbTiO_3$ has a large spontaneous polarization ($75\mu C/cm^2$) high electro mechanical coupling in the C direction (as C axis is the polarization axis) small dielectric constant ($\varepsilon_r \sim 100$) [29 30] and high pyroelectric coefficient ($\rho = 2\,5 \times 10^{-8}$ C cm^2/ K) [4] Therefore it has a large pyroelectric figure of merit (F_V) as

$$F_V = \rho / C_V \varepsilon_r \qquad (1\,11)$$

where C_V = volumetric specific heat

Because of these reasons considerable research efforts are being devoted to produces C axis oriented PT thin films for pyroelectric devices [31 33] Some of the features of the works on the PT thin films are shown in Table 1 3 [5] But with a high paraelectric to

ferroelectric transition temperature ($T_c \sim 490^0$ C) and high tetragonal distortion (c/a ~ 1 06) poling of PT requires high electric field and generates cracks in the films One approach to overcome this problem is by addition of La in PT [34 35]

Table 1 3 A synopsis of some recent work on c axis oriented $PbTiO_3$ thin films [5]

DEVICE STRUCTURE	FEATURE	AUTHORS
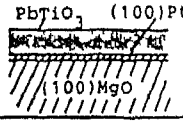	La d ped Large pyro electricity	Iijima et al
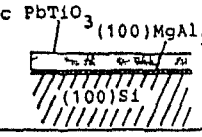	Si substrate	Matsubar et al
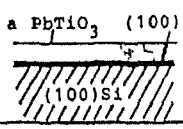	Si ubstrate	Okuyama et al
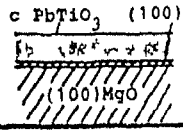	Ca doped Large pyro lectricity	Watanabe et al

Since 1986 work is being carried out on pyroelectric properties of PLT thin films In that year an important work was by K Lijima et al [36] in which rf magnetron method was used to prepare highly C axis oriented PLT thin films with composition $Pb_{1-x}La_xTi_{1-x/4}O_3$ (where x = 0 05 0 10 and 0 15) on MgO single crystal and on epitaxial Pt thin film substrates The results of this study are as follows

1 Degree of C axis orientation of PLT film decreases tetragonality (c/a) decreases and Curie temperature decreases with increasing La content
2 D E hysteresis loops become steep and symmetric with increasing La content
3 The most striking point is that the pyroelectric coefficient (ρ) and dielectric constant (ε_r) increase with increasing La content and at La = 15 ρ is highest (Fig 1 7) But considering the figure of merit (F_v) and temperature coefficient of pyroelectric constant the authors concluded that PLT films with x= 0 10 are good material for pyroelectric IR detector

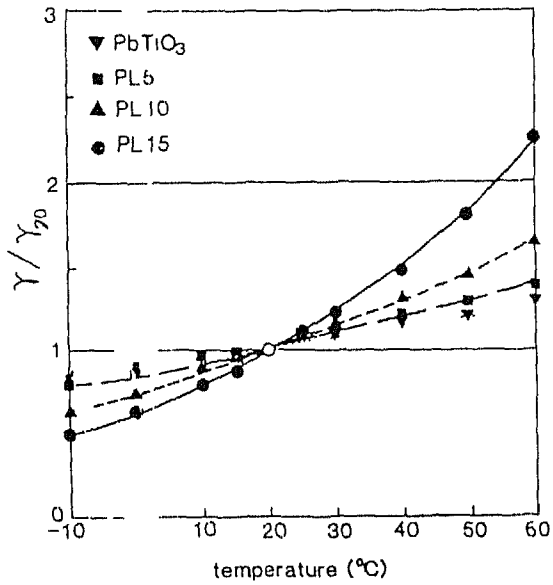

Fig 1 7 Temperature dependence of pyroelectric coefficient (ρ) of the films [36]

In 1990 K Tominaga et al [9] deposited PLT thin film by MOCVD process on MgO (100) The film was highly C axis oriented having the orientation parameter α between 0 8 and 0 9 where α is defined as

$$\alpha = I(100)/[I(001) + I(100)] \qquad (1\ 12)$$

where I (001) and I(100) are the intensities of the corresponding X ray diffraction peaks They also deposited PLT film on Pt/MgO (100) to measure the dielectric properties These films were single perovskite type but not C axis oriented The dielectric constant (ε_r) and loss factor (tanδ) of these films at room temperature were 800 2700 and 0 04 0 10 respectively

Schwartz et al [37] worked on sol gel derived PLT thin films by spin coating method on Pt/Ti/SiO_2/Si substrates They showed that PLT thin films have the following attractive properties

(a) High pyroelectric coefficient (1 5 x 10^{-8} C/cm^2 K)

(b) Conversion to perovskite at a lower temperature than PT and PZT

(c) Unique second order electro optic effects for PLT composition with high La concentration

These workers also notified that with increasing La concentration the dielectric constant increases The properties of same PLT film composition prepared by them are tabulated in Table 1 4 They showed that with increasing La content the hysteresis loops become slimmer and symmetric The decrease in the asymmetry of the loop may be due to the decrease in the internal bias field or in the level of the coupling At 20 at % La the ferroelectric to paraelectric phase boundary (La at % =28) is being approached

Table 1 4 Variation of properties of PLT thin films with different La content [37]

% La	Dielectric constant(ε_r)	Remnant polarization(P_r)	Coercive field (E_C)	Dissipation factor	Curie Point (^{0} C)
0	80	6 6	97 1	0 03	490
5		12 9			-
15					208
20			19 8		140
25	690	1 8		0 087	91

Y Shimizu et al [38] worked on sol gel derived PLT thin film in which La concentration was 18 at % They also deposited the film by spin coating on the 0 02 μm Ti/0 43μm Pt/ SiO_2 substrates They show the variation of the dielectric constant of the films prepared in different ambients (air and pure O_2) (Fig 1 8) with temperature They also compared the effect of thickness of the PLT (18) films on their dielectric constant at different annealing temperature (Fig 1 9) The values of loss (tanδ) for these films vary from 0 013 to 0 055 with temperature

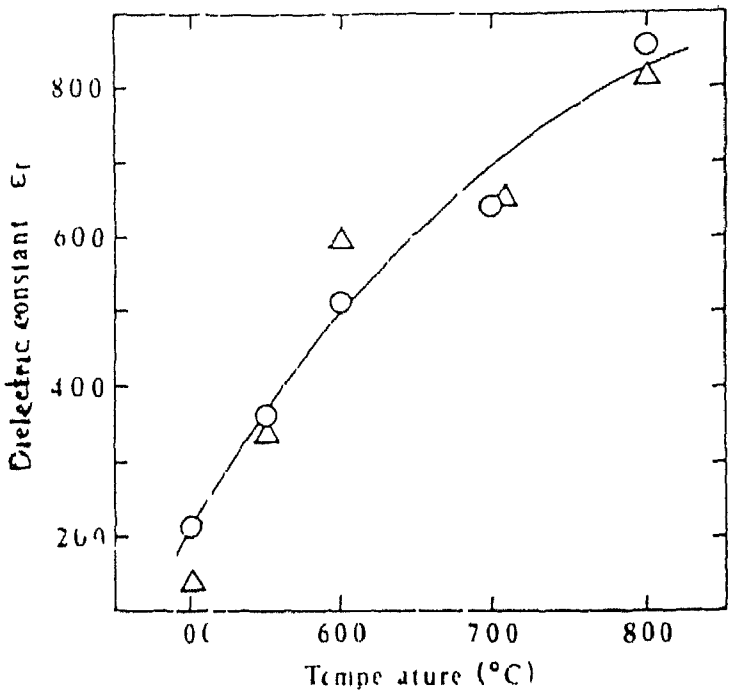

Figure 1 8 Effect of the annealing temperature on the dielectric constant of the PLT (18) thin films with 5 coating (O) fired in air and (Δ) fired in oxygen [38]

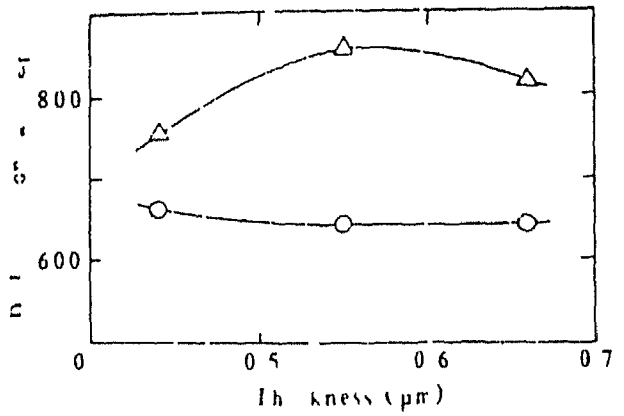

Figure 1 9 Effect of thickness on the dielctric constant of PLT(18) films fired at several temperatures (O) 700^{0}C 3 hr and (Δ) 800^{0}C 3 hr [38]

G R Fox et al [39] worked on the high field electrical properties of ferroelectric thin films They deposited the lead lanthanum titanate (PLT) thin films by multiion beam reactive sputtering (MIBRS) They show that at different applied field the conduction

characteristics of the films can be defined by different mechanism At low field conduction in PLT is ohmic at a critical field it is defined by space charge limited (SCL) current and another mechanism is trap field limited (TFL) They also proved that with increasing La concentration the voltage at which SCL TFL transition occurs increases The electrical characteristic of the films is also explained by means of these mechanisms

N Nagao et al [40] deposited 1 5 μm thick PLT (15) films by rf magnetron sputtering method They used Pt/MgO substrates They studied the effect of the sputtering condition on the films According to their work presence of excess PbO on the growing surface enhance the C axis orientation of the film and its crystallinity The films showed high pyroelectric properties (ρ = 1 3 x 10^{7} C/cm^2 K) low dielectric constant (ε_r = 350) and high figure of merit (F_V =1 2 X 10^{10} C cm/J) much higher than PT (F_V ~ 0 3 x 10^{10} C cm/J) or $PL_{10}T$ (F_V ~ 0 5x 10^{10} C cm/J) thin films They also studied the increase of T_c and broadening of the dielectric phase transition with the variation of La content

H Maiwa et al [41] worked on the ferroelectric fatigue and refreshment of (Pb La)TiO_3 thin films The substrates was Pt/MgO The process of deposition was multiple cathode rf magnetron sputtering When DC bias voltage (20v) was applied on the fatigued sample for 10^4 sec the remnant polarization (P_r) increased On heat treatment (400^0 C) of the fatigued films for 1 hr the coercive field decreased and the sequences of the film improved They could not explain the mechanism of the controlled fatigue property but they thought that defect dipoles may play an important role

H Maiwa et al [42] showed in another paper that crystallinity and Pb content highly effect the ferroelectric properties of the PLT thin films They also compared the effect of the substrates on the electrical properties of PLT According to their work PLT thin films on Pt/MgO substrates show higher crystallinity Square hysteresis loop and higher P_r values compared to the films on $Pt/SiO_2/Si$ substrates At lower temperature (515^0 C) PLT films deposited on the substrates show good ferroelectric properties than the films deposited on the same substrates at the higher temperature (540^0 C)

Adachi et al [43] show that at room temperature the dielectric constant of the PLT (15) film is ~ 1070 So it can be used for the DRAM application They measured the P E hysteresis loop at 60 Hz The loop was asymmetric in nature with P_r and E_c values 8 5 μC/cm^2 and 78 kV/cm respectively They got a high value of pyroelectric coefficient (ρ = 3x 10^{-8} C/cm^2 K) without poling

K Kamachi et al [44] used rf magnetron sputtering method and developed a reproducible preparation method for the preparation of high quality PLT thin films They prepared PLT thin films with very high C axis orientation ($\alpha \sim 1\ 0$) They measured the pyroelectric coefficient (ρ) and dielectric constant (ε_r) as the function of the substrate temperature (T_s) PLT thin films deposited on the substrate of temperature 580^0 C showed the highest pyroelectric coefficient of $4\ 2 \times 10^{-8}$ C/cm^2 K which is twice as much as that of PT The dielectric constant of the PLT films were shown to have very small values (~ 290)

Lee et al [7] investigated the microstructure and electrical properties of $Pb_{0\ 95}La_{0\ 05}TiO_3$ thin films on (100) oriented Pt/MgO substrates by rf magnetron sputtering method They show that if the MgO crystal is fully covered by Pt film then the PLT is not C axis oriented but if Pt films covered the MgO cryatals only partially and formed a percolating network PLT films grow epitaxially along C axis Authors were able to get highly C axis oriented PLT thin films on MgO (100) crystals covered 60 % by sputtered Pt This film showed a hysteresis loop with $P_r \sim 1\ 6\mu C$ / cm^2 and $E_c = 70$ KV/cm Following results were obtained by the workers

Remnant polarization (P_r)	=	1 6 μC/cm^2
Coercive field (E_c)	=	70 kV/cm
Dielectric coefficient (ε_i)	=	80 100
Dissipation factor (tan δ) (at 1 KHz)	=	0 014 0 03
Pyroelectric coefficient (ρ) (without poling)	=	4 5 x 10^{-8} C/cm^2 J
Figure of merit (F_v)	=	1 4 x 10^{10} C c /J

Y M Kang et al [13] prepared the $Pb_{1-x}La_xTiO_3$ (X= 0 28) epitaxial thin films on the Mg (100) and $SrTiO_3$ (001) single crystal substrates by pulse laser deposition method They show that as the La concentration increases the crystal quality improved (better crystallinity) up to x = 0 08 Between $0\ 08<x<0\ 16$ there is no change in the quality and after that it degrades At $x \geq 0\ 20$ a massive thermal stress developed during cooling which could not be relieved by structural transformation as c/a ratio is small and curie temperature is very close to room temperature

In their paper S J Kang et al [10] studied the dielectric and ferroelectric properties of PLT thin films with increasing La content They studied the optical properties also They show that with increasing La content from 15 % to 28 % the hysteresis loops widen slightly Both P_r and E_c decrease with increasing of La from 15 to 28 mole % and then increase The authors concluded the PLT 28 to be the best for DRAM application At 100 Hz frequency the dielectric constant (ε_r) and dielectric loss (tan δ) are 940 and 0 08 respectively The leakage density at 1 5 x 10^5 v is 1 x 10^{-6} amp/cm^2

K Takashi et al [45] compared the intermittent and continuous rf magnetron sputtering deposition method In intermittent deposition method the horizontal grain growth of the films is rapid in the other method Film prepared in this method show higher pyroelectric coefficient (ρ = 5 x 10^{-8}C/cm^2 K) and low dielectric constant (ε_r = 185) as compared to the other methods

K No et Al [11] prepared PLT films by sol gel method The substrate was Pt (1000A^0)/Ti (500A^0)/SiO_2(2000A^0)/Si (100) They obtained the following properties of the films (Table 1 5)

Table 1 5 Electrical properties of PLT thin films with different La content [11]

La content (%)	Film Thickness(nm)	K	E_c(kV/ cm)	% P_r (μC/cm^2)	P(G cm)	ρ(nC/cm^2 K)
0	740	280	161	21	23	1 3
5	680	630	105	27	73	1 9
15	670	870	58	15	95	2 5

Figure 1 10 shows the variation of pyroelectric coefficient with temperature

H Maiwal et al [8] prepared PLT thin film by multiple cathode rf sputtering method They studied the properties of PLT thin films with La content 17 to 28 mole % At lowest La content (La/Ti ~ 0 17) they observed well defined hysteresis loops while at higher La content it behave almost single line Figure 1 11 shows the variation of the dielectric constant with La content variation The dielectric constant and leakage current of 100 nm thick PLT (La/Ti ~ 0 28) thin films were 396 and 10^{-7}A/cm^2 respectively which indicate that the PLT films fabricate by this method are suitable for DRAM application

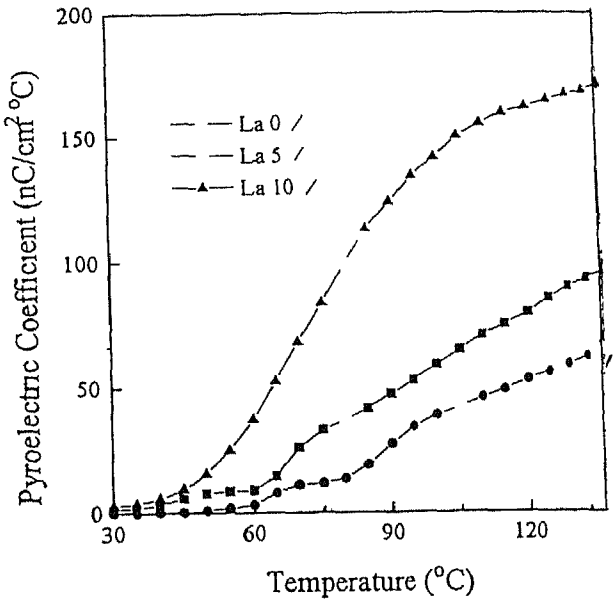

Figure 1 10 Pyroelectric coefficient vs temperature plot of the films with different La content [11]

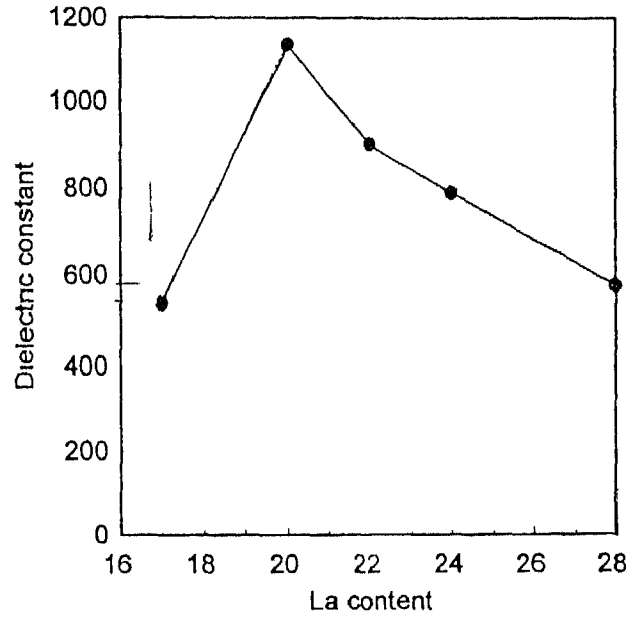

Fig 1 11 Dielectric constant of the 300 nm thick PLT thin films with different La content at room temperature [8]

Many other reports are available in this area [47 51] but K Iijima et al [52] had done an interesting study on the preparation and properties of La modified $PbTiO_3$ thin film They prepared the film by rf magnetron sputtering They shows that PLT thin films with La content 15 mole % has an extremely large pyroelectric coefficient of 9 5 x $10^8 C/cm^2$ K and low dielectric constant of 330

Recently Majumder et al [53] have reported significant enhancement in properties of PZT thin films doped with Ce They prepared PZT and Ce doped PZT thin films on the polished and cleaned polycrystalline Pt substrates They measured the hysteresis loop characteristics and fatigue resistance of the films In both cases addition of Ce had a dramatic effect They showed that upto 1 at % Ce doping the remnant polarization (P_r) and saturation polarization (P_s) values increase and corresponding coercive field (E_c) decreases However above 1 at% Ce doping the polarization values deteriorate and coercive field increase On the other hand hysteresis loops with 1 and 3 at % of Ce show dramatic improvements in resistance of fatigue

According to this discussion PLT thin film act as a promising materials for pyroelectric applications But its ferroelectric properties are poor It has show low values of P_r Ps and high E_c

1 7 Statement of the Problem

Guided by the above discussion we decided to work on Ce doped PLT thin films From journal review it became clear that although PLT thin film is a good pyroelectric material its ferroelectric properties are poor So we planned to study the effect of Ce on the electrical properties of the PLT film As $PL_{15}T$ gives the highest pyroelectric coefficient value we took this material as the starting composition The aim of our work is as follows

1 To study the phases and lattice parameters of the films containing different amounts of Ce
2 To study the electrical properties (ferroelectric and dielectric) of the films
3 To optimize the composition for highest ferroelectric and dielectric properties

Chapter 2

Experimental Procedure

2 1 Preparation of Sample

2 1 1 Formulation

When an additive oxide is added to a material with perovskite structure (ABO_3) of the crystal the added cation distribute itself in between A and B sites in a ratio depending on the size of the coming and substituted cations According to Goldsmidt a cation can be substituted for another cation if the radii of the two cation don t differ by more than 15% Table 2 1 shows the radius of the Pb La Ce and Ti cations According to this Table La^{+3} is within 15% of Pb^{+2} So La^{+3} fully substituted Pb^{+2} and takes place in A site with B site vacancies (for charge balance) For Ce at +3 oxidation state it is within 15% of La^{+3} andPb^{+2} and in cerium trinitrite hexahydrate ($CeNO_3$ $6H_2O$) Ce is in + 3 state So at the beginning it can be said that Ce^{+3} will substituted the La^{+3} mainly Depending on this theory we had calculated the composition of the sol as below which is supported by the works of other scientists [18 27 34 37] also, As PLT thin film with 15 mole % La shows the maximum pyroelectric coefficient [34] we have taken the following composition

$Pb_{1\,05\ 15}La_{15\ x}Ce_x[Ti_{0\,9625}\square_{0\,0375}]O_3$

or

$Pb_{0\,9}La_{15\ x}Ce_x[Ti_{0\,9625}\square_{0\,0375}]O_3$

with x= 0 0 0 3 0 5 0 7 respectively

Table 2 1 Effective ionic radii of La Pb Ti and Ce at different valance states and coordination number [54]

Ions	Goldschmidt(A^0)	Pouling(A^0)	Ahrens(A^0)	Others(A^0)
La^{+3}	1 22	1 15	1 14	XX
Pb^{+2}	1 32	XX	1 20	XX
Ti^{+4}	0 64	0 68	0 68	XX
Ce^{+3}(C N 6)	1 18	XX	1 07	XX
Ce^{+3}(C N 12)	XX	XX	0 94	1 034
Ce^{+4}(C N 6)	1 02	XX	XX	XX

2 1 2 Preparation of Lead Lanthanum Titanate (PLT) and Lead Lanthanum Cerium Titanate (PLCT) Sol

For the preparation of thin films of lead based compounds usually an inorganic salt such as lead acetate is usually used as a source of Pb while other cations are provide by their respective alkoxides Precursors with high metal and low organic content lead to crack free PLT or PLCT thin films after heat treatment because of less volume shrinkage due to removal of organic during firing On the other hand precursors with high metal content are reactive to moisture and are difficult to prepare into a stable sol Again in alkoxides the reactivity of alkyl groups increases with decreasing molecular weight in order of methyl>ethyl>propyl>butyle>higher alkyl groups So a higher order ti butoxide is used for the preparation of PLT and PLCT sol

Many different ways have been reported for the preparation of PLT sol as mentioned earlier In the present case the method used by Yi et al [55] has been used with some modefication The chemicals used are listed in Table 2 2

Table 2 2 Chemicals used for sol preparation

Compounds	Formula	Molecular Weight	Density
Tt 4 Butoxide	$Ti(OC_4H_9)_4$	340 35	0 995
Pb Acetate	$Pb(CH_3COO)\ 3H_2O$	379 33	2 55
La Nitrate Hexahydrate	$La(NO_3)_3\ 6H_2O$	432 9	—
Ce Nitrate hexahydrate	$Ce(NO_3)_3\ 6H_2O$	434 115	—
Acetic acid	CH_3COOH	60 05	1 431
Iso propanol	C_3H_7OH	60 10	0 785
Water	H_2O	18 00	~ 1 00

Lead acetate trihydrate [Pb $(CH_3COO)_2\ 3H_2O$] is mixed with acetic acid in a three necked flask (molar ratio 1 4) and heated in an oil bath (Fig 2 1) to remove the water associated with lead acetate Ideally the water from lead acetate should come out and condense in the condenser But no sign of such condensation is observed This is to be believed due to the following reasons

1 Size of the three necked flask is larger than necessary Only lower portion of the flask gets heated while the upper remains cool The water vapour condenses on the cool part and flows back in to the sol
2 Design of the flask and condenser system system is not proper Very limited amount of vapour entered into the condenser

Proper design and use of small flask may solve this problem However despite this problem sufficient water is removed to yield a stable sol For this the temperature is kept constant at 120^0 C for 15 20 minutes The mixture is cooled to ~90^0C In the mean time ti butoxide is mixed with acetic acid (ti butoxide acetic acid ~ 1 2 mole ratio) in the

glove box and stirred well This mixture is poured down into the three necked flask at ~ 90^0 C and stir for 15 20 minutes Here acetic acid (AcOH) is used for two reasons

1 It acts as a chelating agent for Ti Butoxide and stabilizes it in sol and slows down the gelation process

$$Ti(OBu^n)_4 + AcOH \rightarrow Ti(OBu^n)_3OAc + BuOH \quad (2\ 1)$$

2 AcOH dissolves the lead acetate

After 15 20 minutes when Pb acetate is mixed well with Ti Butoxide sol La $(NO_3)_3\ 6H_2O$ (for PLT sol) or La $(NO_3)_3\ 6H_2O$ + $Ce(NO_3)_3\ 6H_2O$ (for PLCT sol) mixed with 0 5 gm AcOH is poured in it In this stage there forms a white precipitation in the flask (due to flocculation) Addition of 3 4 drops of water restores the clarity of the sol In this last stage sol is stirred for 30 minutes and finally the yellowish transparent and viscous sol is transferred to a polyvinyl container and stored in a vacuum dessicator It is called precursor sol Table 2 3 shows the amounts of the various chemicals used in a typical sol preparation In all cases the sols are prepared to yield 0 01 mole formula unit in 10 ml volume

Table 2 3 Amount of chemicals used for the preparation of 0 01 M sol

Sol formula	$La(NO_3)_3\ 6H_2O$ (gm)	$Ce(NO_3)_3\ 6H_2O$ (gm)	Pb acetate (gm)	Ti butoxide (gm)
$PL_{15}T$	0 65	0 00	3 424	3 276
$PL_{12}C_{03}T$	0 52	0 13	3 424	3 276
$PL_{10}C_{05}T$	0 43	0 22	3 424	3 276
$PL_{08}C_{07}T$	0 347	0 304	3 424	3 276
In all cases the amount of acetic acid mixed with Pb acetate is 2 4 gm and that mixed with ti butoxide is 1 2 gm				

Fig 2 2 shows the flow diagram of the preparation of PLT and PLCT sol

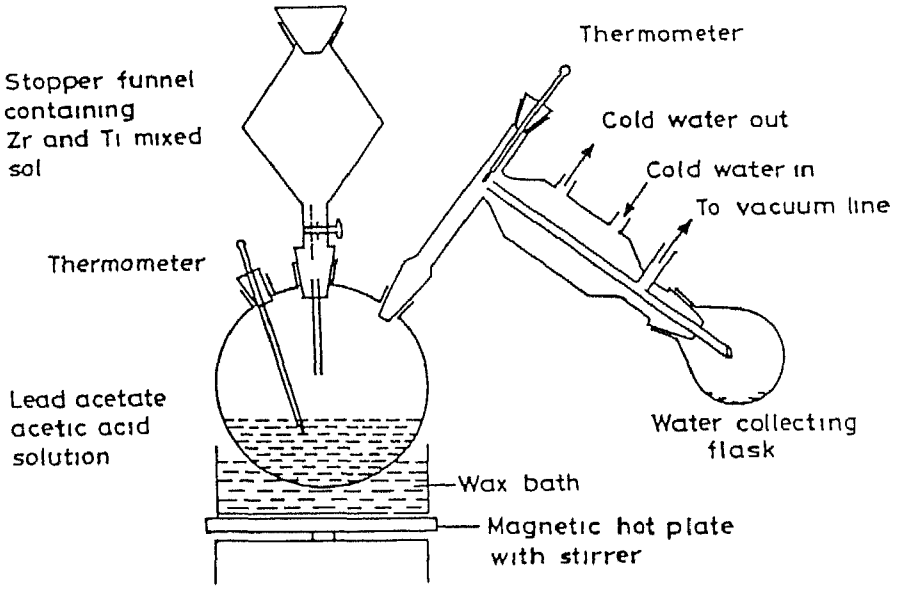

Fig 2 1 Arrangement for sol preparation

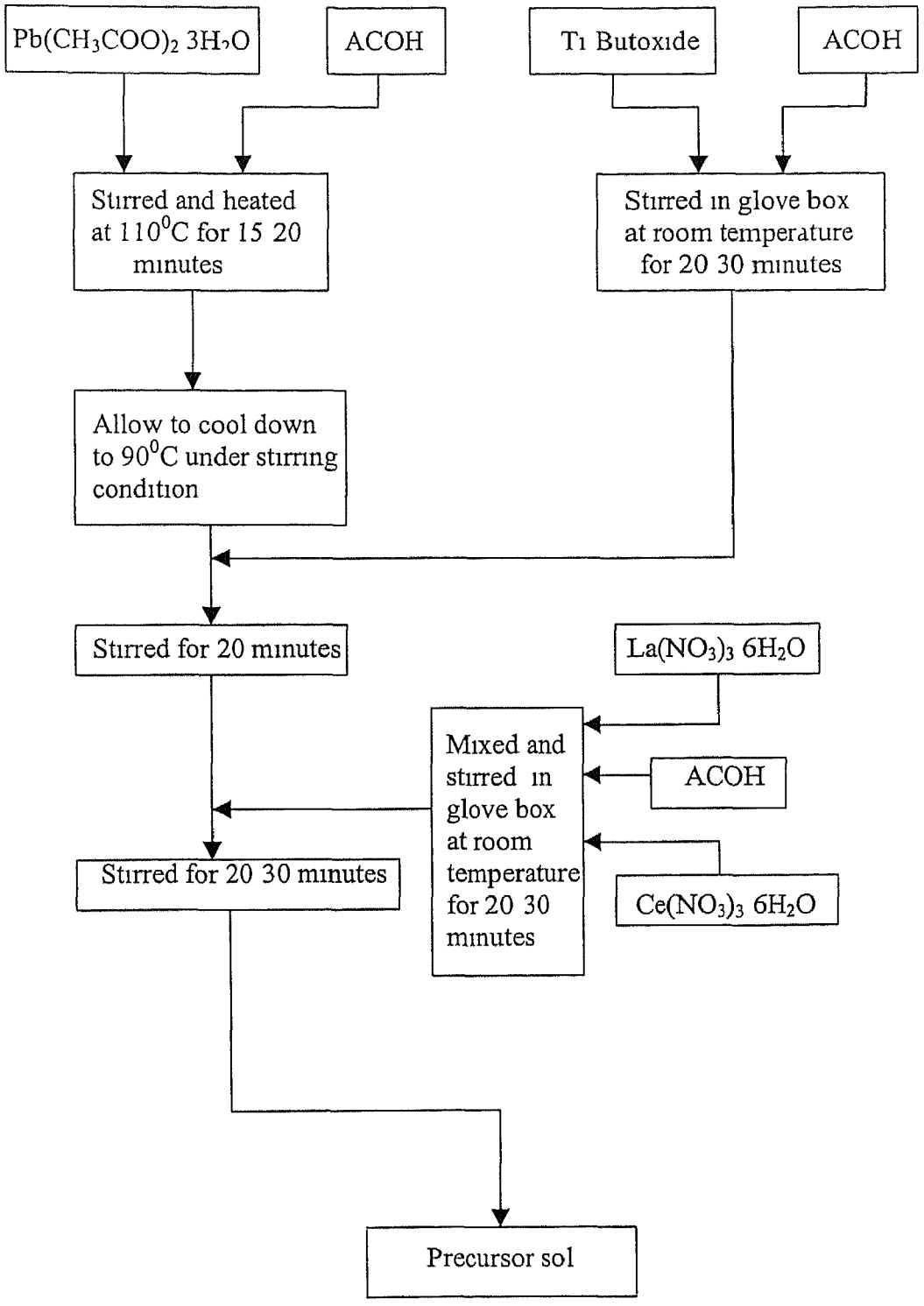

Fig 2 2 Flow diagram for the preparation of PLT/PLCT sol

2 1 3 Substrate Cleaning

Different substrates have been used for the preparation of ferroelectric thin films [4 5 37 9 39 42 7 13 10 11 8 12 55] For phase and microstructural study MgO (100) single crystal epitaxial Pt Si (100) fused quartz sapphire (0001) platinized MgO $SrTiO_3$ etc have been used For electro optic studies glass (corning) coated with transparent and conducting Indium Oxide (ITO) is used For electrical studies platinized Si Si coated with RuO_2 $Pt/Ti/SiO_2/Si$ $Si/TiO_2/Pt$ $Pt/SiO_2/Si$ $Pt/MgO/RuO_2/Ru/SiO_2/Si$ $RuO_2/Ru/MgO$ etc are used In our study polished and polycrystalline Pt substrates as well as sapphire have been used The Pt substrates (10 x 10 x 0 8 mm^3) are first mounted on bakelite stubs and polished on a velvet polishing cloth fixed on a rotating wheel with water suspension of 1 μm Buehler γ Al_2O_3 powder After polishing the substrates are checked in an optical microscope and repolished until free of scratches

Cleaning is the next step of polishing For cleaning the following steps are followed one after another

1 Substrates are ultrasonicated in a 100 ml beaker in soap triple distilled water for a few minutes
2 Substrates are ultrasonicated 4 5 times in triple distilled water until free of polished particles
3 Substrates are washed in acetone for 2 3 times
4 Finally substrates are ultrasonicated with ethanol twice

After cleaning the substrates are allowed to dried in open air and then kept in small plastic container covered with clean cotton The containers are kept in dessicator and used for the film preparation

2 1 4 Preparation of Film

Film is deposited on the cleaned substrates using the precursor sol For film preparation this precursor sol has to be diluted to 0 30 0 25 M with a 1 1 acetic acid and propanol solution For this dilution 1^{st} the volume of the precursor sol is measured by means of a clean and dry measureing cylinder Then the following formula is used for the dilution of the sol

$$S_1V_1 = S_2V_2$$

Where S_1 = Concentration of precursor sol in moles/lit

= (0 01x1000)/10 = 1 M

V_1 = Volume of the precursor sol ~ 10 ml

S_2 = Concentration of dilute sol ~ 0 25 0 30 M/lit

V_2 = Volume of the diluted sol = ?

So V_2 = (10 x 1)/(0 25) = 40 ml

The propanol acetic acid added = (40 10) ml = 30 ml

The sol usually showed some turbidity at this stage Addition of 1 or 2 drops of water removes this turbidity According to Liples et al [57] ratio of the water and total molar concentration of hydrolizable cation should not be more than 0 5

Diluted sol is spin coated on the cleaned Pt and sapphire substrates Research centrifuge (R 24 Remi instruments India) is used for this purpose In spin coating molar concentration of sol spin speed (ω) and duration of spinning determines the film thickness The relation between thickness (t) of the film and spin speed is as follow [58]

$$t = k\omega^n \qquad (2\ 2)$$

where k is a constant which depends on the evaporation rate viscosity and molecular weight of the sol and n is the spin coefficient

In this study a spin speed of ~ 5000 rpm and time of ~ 20 sec is used

2 1 5 Drying and Heating

The spin deposited film on the substrate is still wet Large amounts of solvent remain entrapped in the pores of the film which should be removed by drying During drying the films may crack due to capillary forces set up in the fine pore pocket entrapping solvent [59] This force is higher in narrower pores The pore size distribution can be changed using different pH and water contents for hydrolysis Base catalyst with lowei water contents yield larger pores of uniform distribution Another way to avoid cracking is to add a surfactant [60] in small quantities Acetone and alcohols have lower surface tension than water However their vapour pressures is high and thus evaporate quickly Some drying controlling chemical additives (DCCA) [61] such as formamide or dimethyl formamide oxalic acid and glycol can be added to solvent which cause narrow pore size distribution and reduce differential stresses cause cracking However the problem of cracks is not severe in films of small thickness

A quartz tube furnace is used for the heat treatment of the films with a programmable temperature controller A chromel alumel (K type) thermocouple connected with the temperature controller is kept close to the sample inside the furnace to control the temperature of the furnace After every coating the sample is kept in an alumina boat and inserted into the furnace maintained at a preset temperature It is kept in the furnace for 15 minutes and then quenched to room temperature This cooling and heating cycle is carried out 25 times to produce films of about 1 2 μm thickness This firing of sample is done in oxygen ambient The inlet from the oxygen gas cylinder is connected to one end (gas inlet) of the quartz tube and other end (gas –outlet) is dipped into water through a rubber tube Gas flow rate is controlled roughly by counting the gas bubbles released per minute through water After the final firing the coated sample (25 coats) is annealed at a higher temperature

Majumder [62] have proposed two types of heat treatment

1 Firing at 400^0 C and then annealing at 700^0 C – that is called low intermediate temperature rapid firing (lirf)

2 Firing at 600^0 C and annealing at 700^0 C – that is called higher intermediate temperature rapid firing (hirf)

Fig 2 6 shows both types of heat treatment schedule

In case of lirf due to firing at low temperature there form a number of nucleation sites but crystallization does not occur When this film is annealed finally at 700^0C small and uniform grained film forms In case of hirf the crystallization start with the formation of nucleation sites at intermediate temperature 600^0 C so that a microstructure of relatively large and nonuniform grain sizes and distribution can be expected

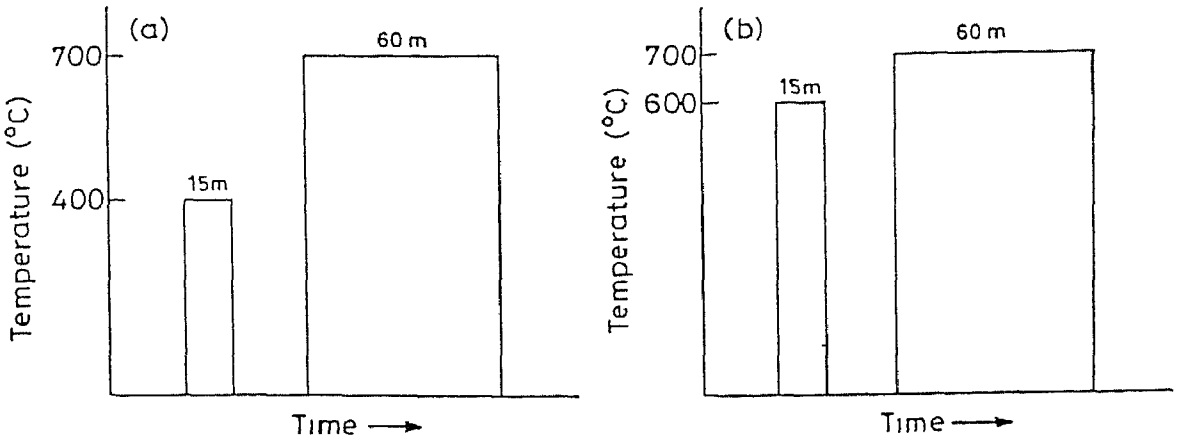

Fig 2 3 (a) Low intermediate rapid fired (lirf) and (b) high intermediate rapid fired (hirf) heating schedule

2 1 6 Film Preparation for TTT Diagram

The as deposited films are amorphous and after heat treatment turn into perovskite crystalline structure from amorphous But there is the possibility of pyrochlore phase to exist as the intermediate phase which depends on the rate of heating temperature of heating time of heating substrate nature ambient etc For studying the effect of temperature and time the PLT thin film of composition $Pb_{0\,9}La_{0\,15}[Ti_{0\,9625}\square_{0\,0375}]O_3$ is prepared separately by the same sol gel technique It is deposited on the polished and cleaned polycrystalline Pt substrates by spin coating method similarly Just after every deposition the films are directly inserted into the quartz furnace preheated at 300^0 C and held for 15 minutes in O_2 ambient After heating the film is quenched in room temperature This heating and coating cycles are repeated for five times Then the film is annealed in temperature varied from 350^0C to 500^0 C and annealing time varied from 1 min to 60 min respectively After annealing the films are quenched in to air The phases are determined by X ray diffraction study

2 2 Characterization

2 2 1 Measurements of Electrical Properties

Polarization vs electric field hysteresis loop and frequency dependent dielectric constant and dielectric loss of the films are measured

Gold palladium (Au Pd) electrodes of 0 05 cm diameter are deposited on the film by means of D C sputtering (Hummer VIA sputtering unit) perforated (0 05 cm) thin aluminum sheet musk of the film The parameters used during sputtering are given in the Table 2 4

Table 2 4 Operating parameters for sputtering deposition of electrodes

Parameters	Value
Gas used	Ar
Gas pressure	55 70 mtorr
Voltage	< 5V
Current	10 amp
Time	10 15 min

Fig 2 4 shows the sample configuration for electrical measurement

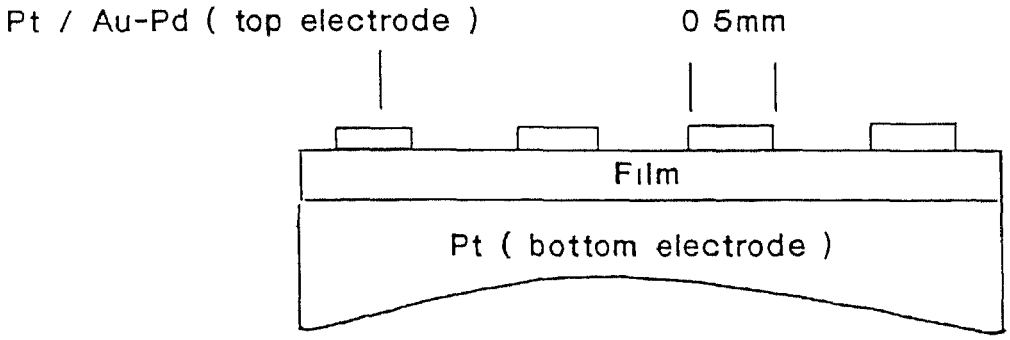

Fig 2 4 Sample configuration for electrical measurement

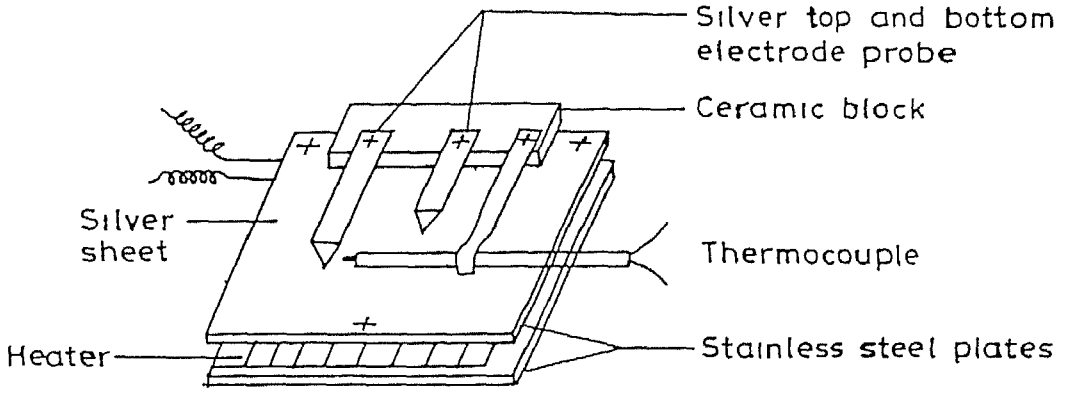

Fig 2 5 Sample Holder

The schematic diagram of the sample holder used for the measurement of the electrical properties is shown in Figure 2 5 [62] It is made of two stainless steel plates A mica sheet wound with a heating coil is positioned in between these steel plates insulated from the coil The upper stainless steel plate is partially covered by 0 2 mm thick silver foil Two pointed silver probes (top and bottom) insulated from each other are fixed on the silver foil A thermocouple can be also kept near the film to measure its temperature during high temperature measurements This sample holder can be used up to 250^0 C

2 2 1 1 Hysteresis Loop Measurement

Change of polarization (P) with applied electric field (E) is the most important measurement for the ferroelectric materials This yields the characteristic hysteresis lop It is measured by Sawyer Tower circuit shown in figure 2 6 Here the film acts as a capacitor and it is in series with an integrating capacitor C The capacitance C is selected to be much higher than the sample capacitance to allow most of external voltage to be applied at the sample The voltage appearing across the integrating capacitor is directly proportional to the surface charge and hence the polarization of the ferroelectric capacitor So by connecting the top and bottom electrodes to an oscilloscope we can observe the hysteresis loop of the sample

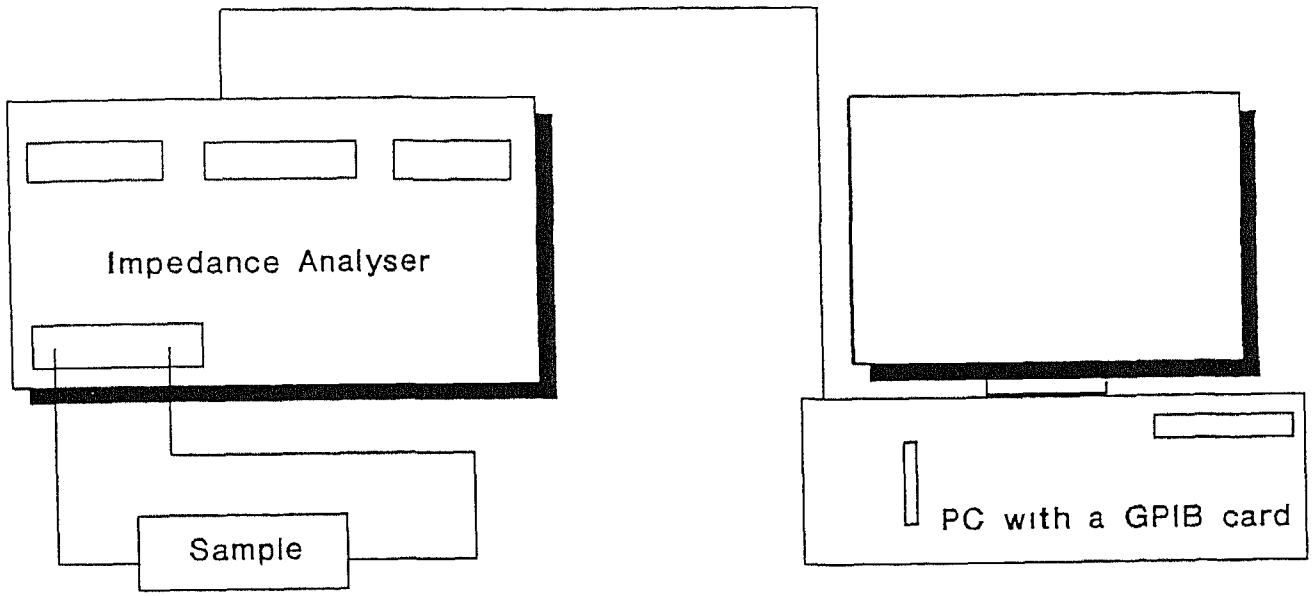

Fig 2 6 The Sawer Tower Circuit

The polarization charge and field across the sample can be calculated from the relation

$$P = CV_i/A \ (\mu C/cm^2) \quad (2\ 3)$$

$$E = V_i/t \ (KV/cm) \quad (2\ 4)$$

Where A = Area of the dot electrode on the film

t = Thickness of the film

V_i = Voltage across the film

2 2 1 2 Dielectric Measurements

The dielectric constant (ε_r) and the dielectric loss factor (tan δ) are measured using an impedance analyzer (HP 4192A) The frequency is varied from 1 kHz to 1 MHz The

change of capacitance is measured with the change of frequency and from this capacitance the dielectric constant is calculated using the formula

$$\varepsilon = Cd/\varepsilon_0 A \qquad (2\,5)$$

where ε_0 = Permittivity of vaccum

d = Thickness of the film

A = Area of the electrode

C = Capacitance

Loss factor is displayed directly by the instrument

2 2 2 X-Ray Analysis

The X ray diffraction of the film is carried out to detect the phases and to calculate the lattice parameters For this purpose we used an X ray diffractometer (Rich Seifert Iso Debyeflex 2002 Germany) CuKα radiation (λ = 1 5405A^0) is used with a Ni monochromator Table 2 5 shows the operating conditions used

Table 2 5 Operating parameters for X ray diffraction

Characteristics	Values
Accelerating Voltage	30 kV
Accelerating current	20 mA
Scanning speed (ss)	3^0/min
Chart speed	3 cm/min
Time constant(T_c)	10 sec
Counts per minute(CPM)	5 K
Range of Scanning	20^0 60^0

The value of d the interplaner spacing is used to calculate the index of the corresponding phases The d value was calculated from the Bragg s law

$$n\lambda = 2d\sin\theta \qquad (2\,6)$$

where θ = Bragg s angle

n = Order of diffraction here n is taken as 1

λ= X ray wave length (~ 1 54 A^0)

For the tetragonal system the lattice parameters have been calculated [63] using the following formula

$$1/d^2 = (h^2 + k^2)/a^2 + l^2/c^2 \qquad (2\ 7)$$

where h k l = Miller indices of the tetragonal system

The 1st step is to calculate approximate values of $\mathbf{a}_1$ and $\mathbf{c}_1$ the lattice parameters from the positions of the two highest angle lines The approximate axial ratio $\mathbf{c}_1/\mathbf{a}_1$ is then calculated and used in equtıon 2 8 to determine **a** values for each high angle line on

$$a = \frac{\lambda}{2Sin\theta}\left[(h^2 + l^2) + \frac{l^2}{(c/a)}\right]^{1/2} \qquad (2\ 8)$$

the pattern These values of **a** are then extrapolated against $\cos^2\theta$ to find a more accurate

$$c = \frac{\lambda}{2Sin\theta}\left[\left(\frac{c}{a}\right)^2 (h + l^2) + l^2\right]^{1/2} \qquad (2\ 9)$$

value of **a** say $\mathbf{a}_2$ The value of $\mathbf{c}_2$ is found in similar fashion by use of the equation 2 9 and again it extrapolate against $\cos^2\theta$ The process is repeated with the new value of the axial ratio $\mathbf{c}_2/\mathbf{a}_2$ to yeild more accurate values of the parameters $\mathbf{c}_3$ and $\mathbf{a}_3$ Generally 5 6 extrapolations are enough to find out almost exact value of the lattice parameters We use a programme (appendix A) to make these calculations

Chapter 3

Results and Discussions

In this chapter we first discuss the X ray diffraction data of the PLT and PLCT thin films in detail Then we discuss the TTT diagram of PLT films In the second part we discuss the electrical properties i e hysteresis loops and dielectric properties of the films Finally we tried to optimize the properties of the samples and draw the conclusion

3 1 Phases in the films

The phases present in the films are determined by X ray diffraction Fig 3 1 and 3 2 show the X ray diffractograms for the films with Ce/La ratios equal to 0/15 03/12 05/10 and 07/08 on Pt and sapphire substrates respectively Table 3 1 and 3 2 give the peak positions (from Figs 3 1 and 3 2) indexed for PLT films according to the data from literature summarized in Table 3 3 [56 37 38 10 12] Table 3 4 gives the data for $PbTiO_3$ from JCPDS files It may be noted that the data summarized in Table 3 3 are obtained for films prepared by different methods and subjected to different heat treatments

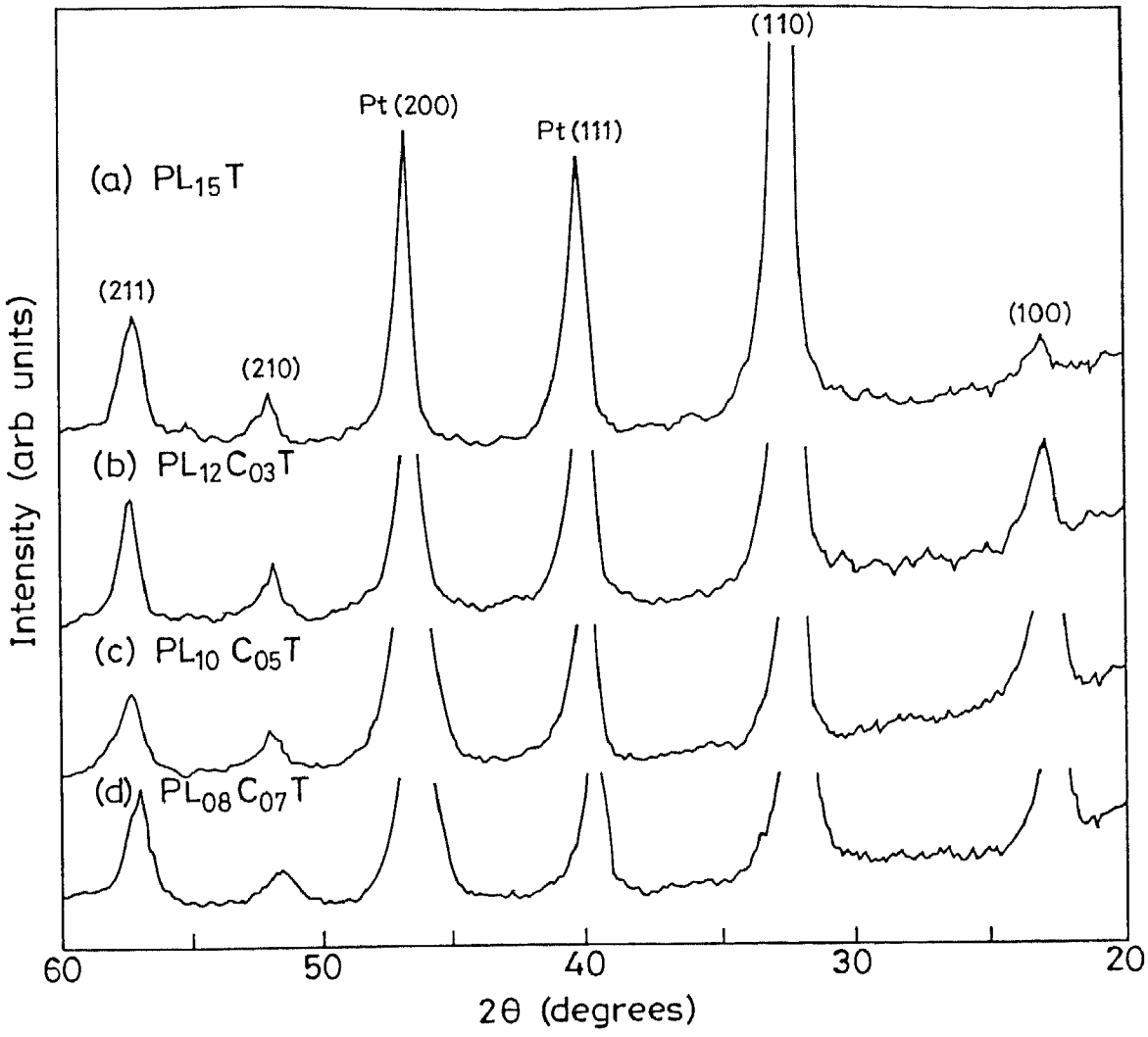

Figure 3 1 X ray diffractogram of the films (a) $PL_{15}T$, (b) $PL_{12}C_{03}T$ (c) $PL_{10}C_{05}T$ and (d) $PL_{08}C_{07}T$ on Pt substrate

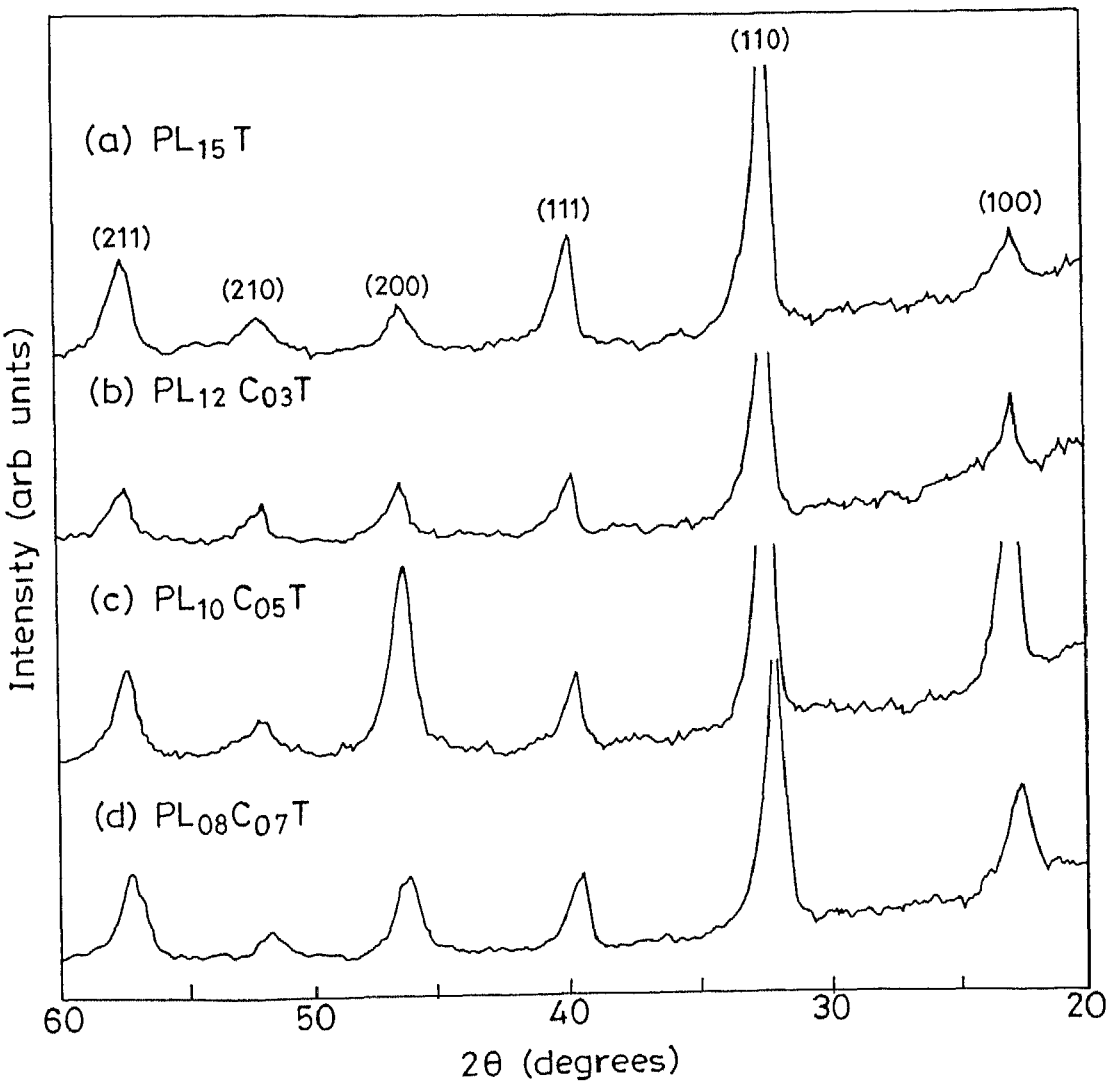

Figure 3 2 X ray diffractogram of the thin films (a) $PL_{15}T$ (b) $PL_{12}C_{03}T$ (c) $PL_{10}C_{05}T$ and (d) $PL_{08}C_{07}T$ on sapphire substrate

Table 3 1 Summary of X ray diffraction data for films on Pt-substrates all films have the perovskite structure data is for two sets of samples

2θ for the films				hkl
$PL_{15}C_0T$	$PL_{12}C_{03}T$	$PL_{10}C_{05}T$	$PL_{08}C_{07}T$	
22 6 22 7	22 8 22 5	22 5 22 6	22 5 22 6	100
32 4 32 1	32 4 32 0	32 0 32	32 0 32 0	110
39 1 39 9	39 0 39 8	39 1 39 8	39 1 39 7	111
46 0 46 4	46 2 46 2	46 0 46 3	46 0 46 1	200
52 0 52 0	57 1 51 7	51 9 51 7	51 7 51 6	210
57 3 57 4	57 0 57 0	57 2 57	57 1 57 0	211

Table 3 2 Summary of X ray diffraction data for films on sapphire substrates all films have the perovskite structure

2θ values for the films				hkl
$PL_{15}C_0T$	$PL_{12}C_{03}T$	$PL_{10}C_{05}T$	$PL_{08}C_{07}T$	
22 75	22 7	22 7	22 5	100
32 25	32 2	32 2	31 9	110
39 6	39 6	39 6	39 5	111
46 4	46 35	46 35	46 15	200
52 1	52 0	52 0	51 9	210
57 4	57 3	57 3	57 2	211

Table 3 3 Summary of X ray data from references[37 38 10 12 55] for PLT thin films

Ref	Substrate	% mole La	Thickness (nm)	2θ	(hkl)	Phase
[38]	Pt/Ti/SiO_2/Si	18		22	100	Perovskite
				29	331	Pyrochlore
				32	110	Perovskite
				46	200	Do
				52	210	Do
				57	211	Do
[37]	Pt/Ti/SiO_2/Si	10	410	20	–	Pyrochlore
				22	100	Perovskite
				32	110	Do
				39 3	111	Do
				46 3	200	Do
				52 3	210	Do
				57 7	211	Do
[55] 6	Pt/Ti/SiO_2/Si	8	>300	22 5	100	Perovskite
				32 0	110	Do
				39	111	Do
				46	200	Do
				52	210	Do
				57	211	Do
[10]	Pt/Ti/SiO_2/Si	15 21 28 33	480	22	100	Perovskite
				32	110	Do
				40	111	Do
				46	200	Do
				52	210	Do
				57	211	Do
[12]	Si(110)	05 10 15	–	22	100	Perovskite
				32	110	Do
				39	111	Do
				47	200	Do
				52	210	Do
				57	211	Do

Table 3.4: X-ray diffraction data for $PbTiO_3$ (PT) thin film from JCPDS file

6-0452 MINOR CORRECTION

d	2.64	2.76	3.90	4.15
I/I1	100	55	50	35

$PbTiO_3$

LEAD TITANATE

Rad. CuKα λ 1.5405 Filter Ni
Dia. Cut off Coll.
I/I1 DIFFRACTOMETER d corr. abs.?
Ref. SWANSON ET AL., NBS CIRCULAR 539 VOL V (1955)

Sys. TETRAGONAL S.G. P4/mmm (129)
a 3.899 b c 4.1532 A C 1.0651
α β γ Z 1
Ref. IBID.

ε nωβ εγ Sign
2V Dx 7.97 mp Color YELLOW-BROWN
Ref.

SPECT. ANAL. OF SAMPLE: <0.1% Si; <0.01% Al, B, Ca, Cu, Fe, Mg, Sn; <0.001% Ag.
X-RAY PATTERN AT 26°C. PEROVSKITE TYPE STRUCTURE

d Å	I/I1	hkl	d Å	I/I1	hkl
4.15	35	001	1.237	4	113
3.90	50	100	1.2333	8	310
2.842	100	101	1.1819	10	311
2.758	55	110	1.1484	6	222
2.297	40	111	1.1287	4	203
2.076	16	002	1.1016	2	302
1.950	30	200	1.0841	8	213
1.833	14	102	1.0816	4	320
1.765	10	201	1.0601	10	312
1.744	12	210	1.0465	8	321
1.6581	20	112	1.0383	2	004
1.6075	40	211	1.0031	2	104
1.4213	14	202	0.9762	4	225
1.3841	4	003	.9747	4	400
1.3787	10	220	.9715	2	114
1.3351	8	212	.9593	4	322
1.3081	4	221	.9491	2	401
1.3045	6	103	.9476	2	303
1.3000	12	300	.9457	4	410
1.2403	10	301	.9222	6	411

In general in the fabrication of ceramic films by the chemical methods crystallization temperature of the film is kept slightly higher than the decomposition temperature of the precursors So the crystallization temperature depends on the precursors used In the present study the films had been finally treated at 700^0 C in oxygen ambient to get complete crystallization and fully perovskite phase

In contrast to the X ray diffractogram for PT film (Fig 3 3) X ray diffractograms for $PL_{15}T$ thin films (Fig 3 1 and 3 2) show no peak splitting for the (100 001) or (101 110) peaks The 2θ values observed for the (001 or 100) and (101 or 110) diffraction peaks of PLT thin films are intermediate to the (100 001) and (110 101) diffraction peaks of PT films Similar observation has been reported by others [37 42 10 12 55 46] also It has been suggested that the PLT thin film is possibly pseudo cubic in nature

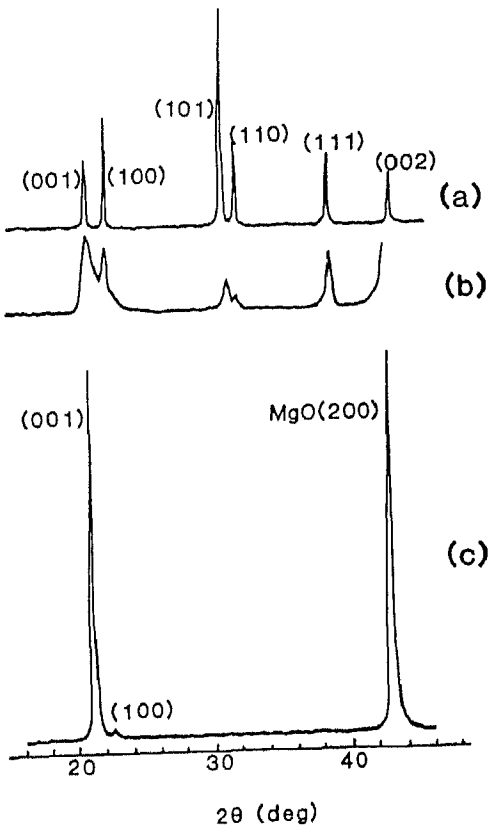

Figure 3 3 X ray diffraction pattern of (a) $PbTiO_3$ powder (b) $PbTiO_3$ film sputter deposited at 10 Pa gas pressure and (c) C axis oriented $PbTiO_3$ film sputter deposited at 1 Pa gas pressure [4]

Nature of the X ray diffractogram of the PLT and Ce doped PLT thin films are almost same However the relative intensity of the peaks changes significantly with composition indicating texture effects Table 3 5 and 3 6 show the variation of the relative intensities (I/I_0) for different compositions of PLCT films

Table 3 5 Variation of I/I_0 for PLT films with different compositions on Pt substrate

Index	I/I_0 for the films			
	$PL_{15}C_0T$	$PL_{12}C_{03}T$	$PL_{10}C_{05}T$	$PL_{08}C_{07}T$
001 100	4 1 14	20 28	63 75 9	40 49 9
101 110	100 100	100 100	100 100	100 100
210	3 74 11	5 55 11 8	09 09	07 11
211	13 23 6	18 16 25	23 19 5	14 7 21

Table 3 6 Variation of I/I_0 for PLCT films of different compositions on sapphire substrate

Index	I/I_0 values of the peaks			
	$PL_{15}C_0T$	$PL_{12}C_{03}T$	$PL_{10}C_{05}T$	$PL_{08}C_{07}T$
001 100	15	30	66	34 8
101 110	100	100	100	100
111	27 4	26 4	23	27
002 200	11 3	22 2	53	26
210	7 5	11	10	08
211	26 4	19 4	27	28

On Pt the (111) and (200) peaks coincide with the (111) and (200) peaks of Pt-substrate so that the I/I_0 values for these two peaks could not be determined

Presence of preferred orientation (texture) in the films depends on various factors like the substrate temperature [40] nature of substrate [42] process of deposition ambient [61] etc Films with (001) texture are preferred for pyroelectric and piezoelectric applications because of their high pyroelectric coefficient and low dielectric constant in the c direction The composition of a film can significantly affect its texture Y M Kang et al [13] showed that for the pulse laser deposited PLT thin films the degree of c axis orientation 90^0 domain configuration and the quality of the crystals depends on the La concentration With the La concentration in between 12 to 16 at % the films show fully c axis orientation From Table3 5 and 3 6 and Fig 3 4 it can be observed that with the initial increase of Ce concentration the c axis orientation of the films increase Above 5 at % Ce this trends is reversed and the c axis orientation of the films decreases From Fig 3 4 it can be see that the data is quite reproducible and does not depend on the nature of the substrate

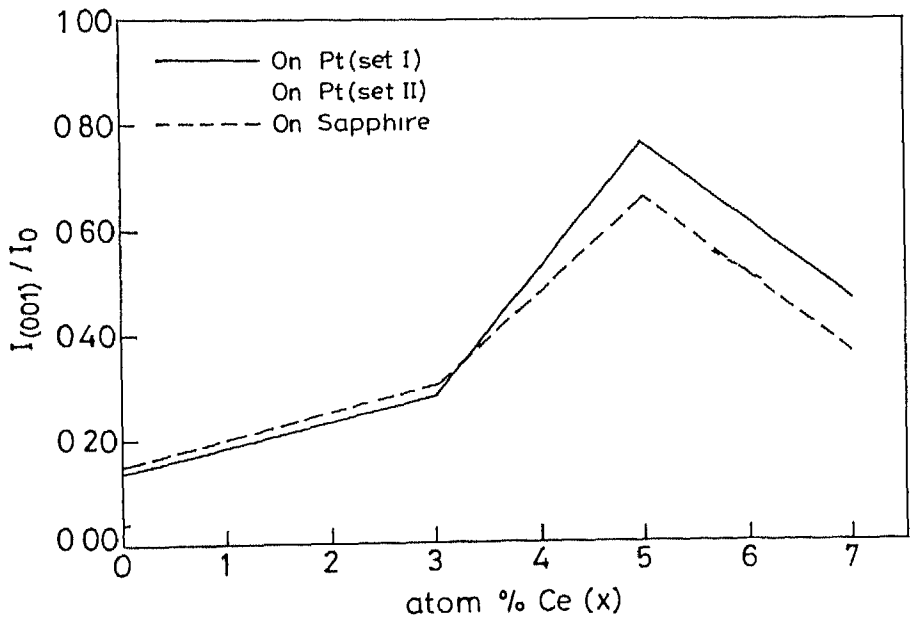

Figure 3 4 Variation of $I_{(001)}/I_0$ with Ce atom % on (a) and (b) Pt substrates and (c) sapphire substrate

3 2 Lattice Constant

As described in chapter 2 attempt has been made to determine the lattice parameters using the (211) (210) (110) and (100) peaks The results are given in Table 3 7 It is seen that the result are not accurate as c/a <1 is obtained More experiments are

Table 3 7 Lattice parameter for the films

Film	c(A^0)	a(A^0)	c/a
$PL_{15}C_0T$	3 97	4 02	0 99
$PL_{12}C_3T$	4 12	4 07	1 01
$PL_{10}C_{05}T$	3 92	3 97	0 99
$PL_{08}C_{07}T$	3 99	3 96	1 01

needed to determine the lattice parameters Data from literature [13] is summarized in Table 3 8 for comparison

Table 3 8 Variation of the lattice parameters with the variation of La concentration [24]

La conc	c(A^0)	a(A^0)	c/a
0 00	4 117	3 925	1 049
0 04	4 060	3 926	1 034
0 08	4 097	3 929	1 030
0 12	4 018	3 932	1 022
0 16	4 026	3 931	1 024
0 20	3 981	3 929	1 013
0 24	3 970	3 927	1 011
0 28	3 959	3 917	1 011

3 3 TTT Diagram

As mentioned earlier the films are dried at 300^0 C after successive coatings To determine the TTT diagram after the final drying step the films are isothermally treated at different temperatures for different times and the resulting phases are determined

Fig 3 5 shows the X ray diffractogram of the PLT film treated at 400^0 C for 60 minutes In this case the film is fully amorphous in nature Similar was the case for the film annealed for 10 minutes This observation is contradictory to the result obtained by Schwartz et al [37] They worked on PLT (La 10) film and showed that the film becomes almost fully perovskite at 400^0C However their substrates and the precursor reactants for the sol preparation were different from our case

Fig 3 6(a to c) shows the X ray diffractograms of PLT film treated at 450^0C for 10 minutes 30 minutes and 60 minutes respectively After 10 minutes treatment at 450^0C two peaks appear at 29 2^0 and at 57^0 Peak at 29 2^0 is most probably due to the pyrochlore phase $Pb_2Ti_2O_6$ [38] and the peak at 57^0 (211) indicates the starting of the perovskite formation in the PLT film After 30 minutes annealing at 450^0 C there is present a broad peak at 31 9^0 which is the peak for perovskite (110) The peak due to the pyrochlore phase has disappeared After annealing for 60 minutes at 450^0 C the film is fully perovskite

Fig 3 7(a to c) show the X ray diffractograms of the PLT film annealed at 500^0 C for 1 minutes 10 minutes and 60 minutes respectively After 1 minutes the PLT film crystallizes partially Only the (110) perovskite peak is present and no pyrochlore peak appears The film crystallizes fully into perovskite phase after annealing for 10 minutes

The X ray data of the isothermal treatments is summarized in Table 3 9 Based on this data a TTT diagram for the PLT thin film has been constructed and is shown in Fig 3 8 The corresponding TTT diagram of PZT thin films determined by Majumder [64] is shown in the Fig 3 9 It is seen that the PLT film crystallizes at much lower temperature than the PZT thin film prepared under similar condition In the PLT film formation of the pyrochlore phase is restricted to a very small region in the TTT diagram and it persists only for a small time Thus La favors early crystallization and formation of the perovskite phase

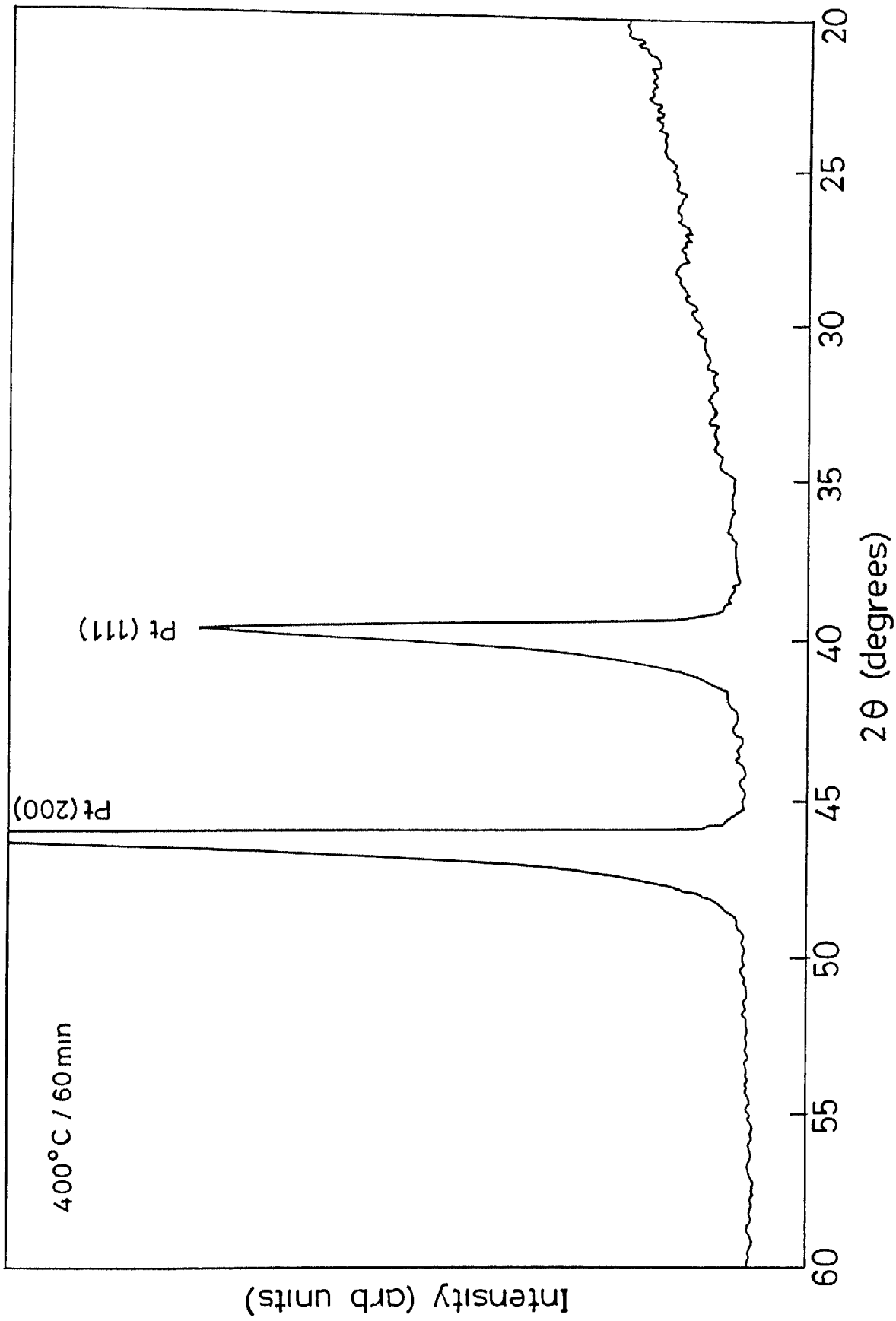

Figure 3 5 X ray diffractogram of $PL_{15}T$ thin film annealed at 400^0C for 60 min

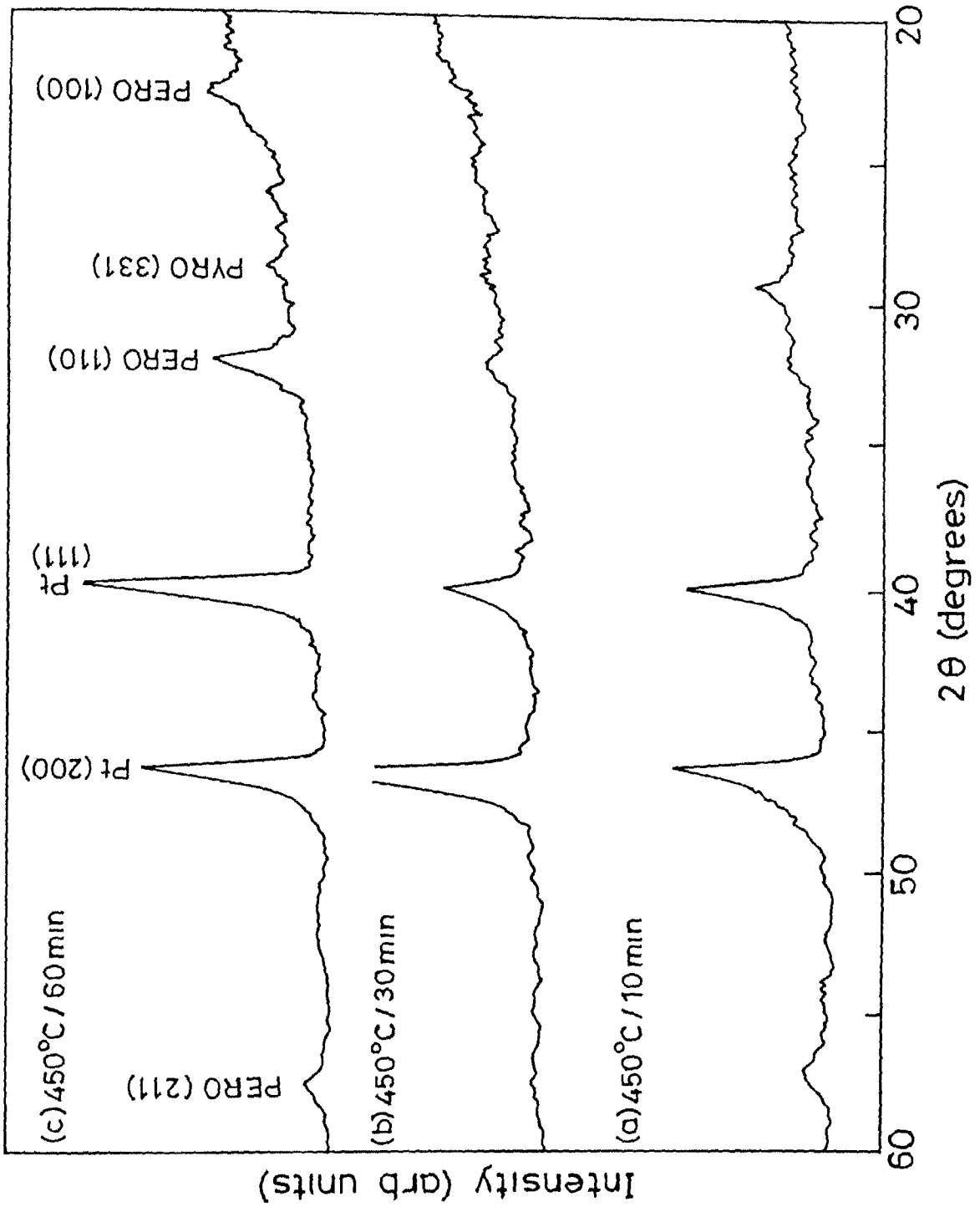

Figure 3 6 X ray diffractogram of $PL_{15}T$ thin film annealed at 450^0C for (a) 10 min (b) 30 min and (c) 60 min

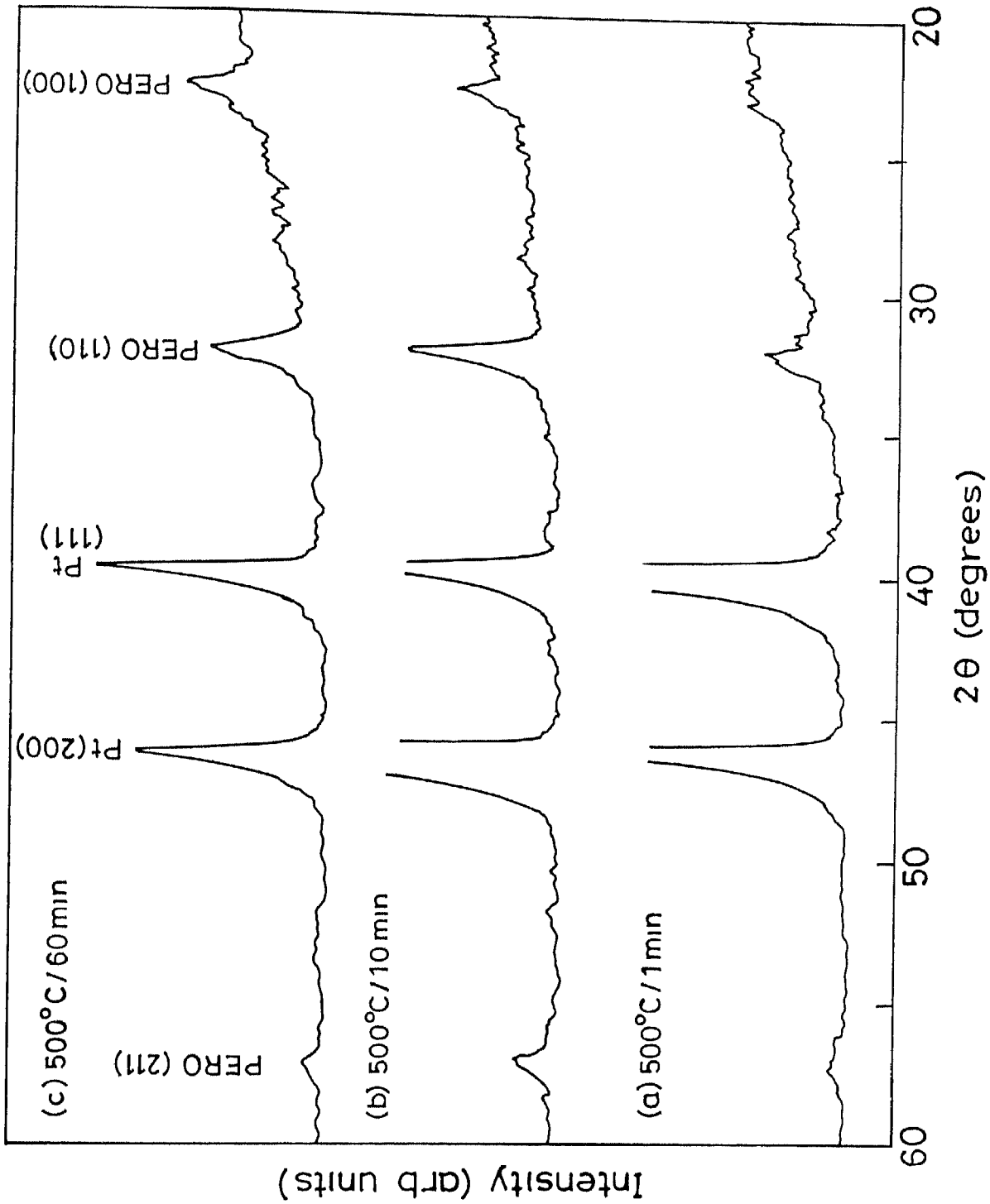

Figure 3 7 X ray diffractogram of $PL_{15}T$ thin film annealed at 500^0Cfor (a) 1 min (b) 10 min and (c) 60 min

Table 3 9 Phases of $PL_{15}T$ films detected by X ray diffraction after different isothermal treatments

Temp(^{0} C)	Time(min)	Phase(s)
350	60	Amorphous
400	10	Amorphous
	60	Amorphous
450	1	Amorphous
	10	Pyro Pero Am
	30	Am Pero
	60	Perovskite
500	1	Am Pero
	10	Perovskite
	60	Perovskite

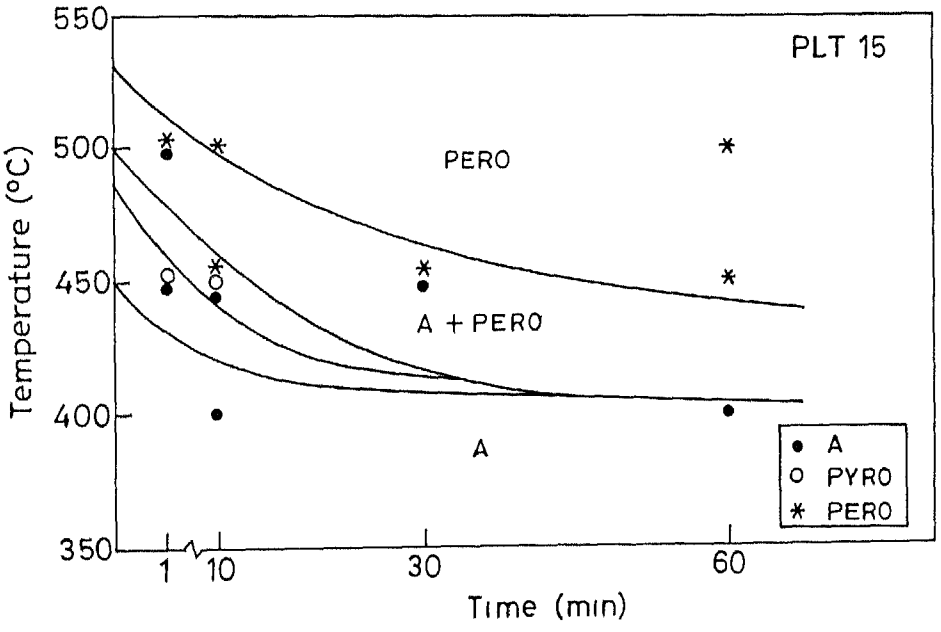

Figure 3 8 TTT diagram of $PL_{15}T$ thin film

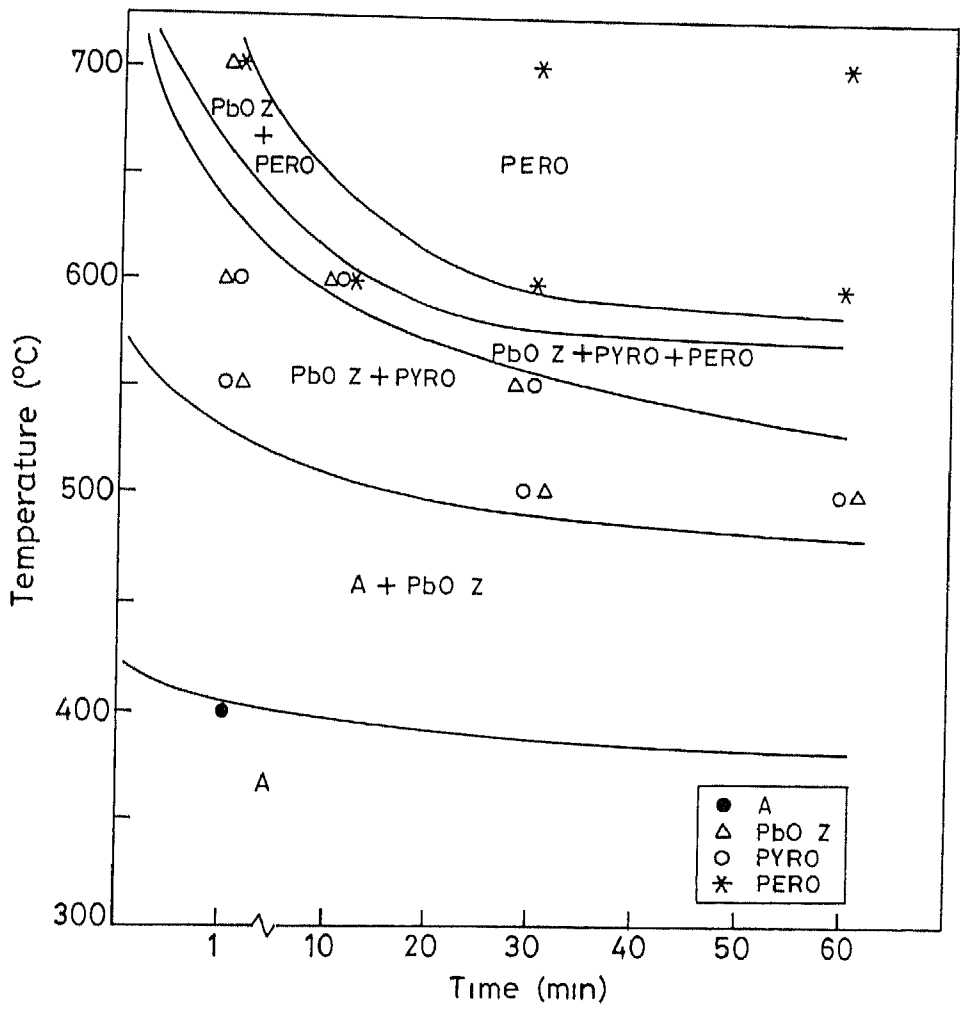

Figure 3 9 TTT diagram of PZT thin film [63]

3 4 Electrical Properties

In this section we first discuss the ferroelectric hysteresis loops for the $PL_{15}T$ and PLCT thin films and their relative properties Secondly we discuss the dielectric properties of the films

3 4 1 Study of Ferroelectric Properties

Substantial amount of data has been reported in literature for $PL_{15}T$ films We first present our results for $PL_{15}T$ films (15 at % La and 0 at % Ce) and compare these with the data from the literature A collection of hysteresis loops for $PL_{15}T$ films is shown in Fig 3 10 The values of the parameters P_s (Saturation Polarization) P_r (Remnant Polarization) and E_c (Coercive Field) measured from these hysteresis loops are given in Table 3 10 Similar data from literature is presented in Table 3 11

Ferroelectric properties of thin films depends on substrate material heat treatment condition precursor used etc Furthermore in the same film the characteristics may change from one device to another depending on the orientation of the crystals grain size defects, microstructure etc

In the data summarized in Table 3 11 a large variation in P_s P_r and E_c are observed P_s is found to vary from 6 to 46 $\mu C/cm^2$, P_r from 2 to 36 $\mu C/cm^2$ and E_c from 31 to 115 kV/cm No trend is apparent dependant on the method of preparation (sol gel or sputtering) The values for our samples (Table 3 10) are $P_s \approx 24 \mu C/cm^2$ $P_r \approx 15 \mu C/cm^2$ and $E_c \approx 52$ kV/cm These values are agree well with the values reported in literature as summarized in Table 3 11

The average values of P_r for the $PL_{15}T$ films (Table 3 10) are consistent with the values obtained by Nagao et al [40] and Meidong et al [64] But the values of E_c of $PL_{15}T$ (Table 3 10) is much lower than the observation of Nagao et al [40] Their observed value of E_c (115 kV/cm) is about four times higher than that of Iijima et al [36] which suggests the existence of a large internal stress developed in the films due to the difference in expansion coefficients between the $PL_{15}T$ thin films and the substrates

Kang et al [10] prepared $PL_{15}T$ thin films on the substrate with composition $Pt(1500A^0)/Ti(1000A^0)/SiO_2(1000A^0)/Si(100)$ using Sol Gel method They used air as the ambient and annealed the film at 650^0C for 30 minutes The P_s P_r and E_c values of their

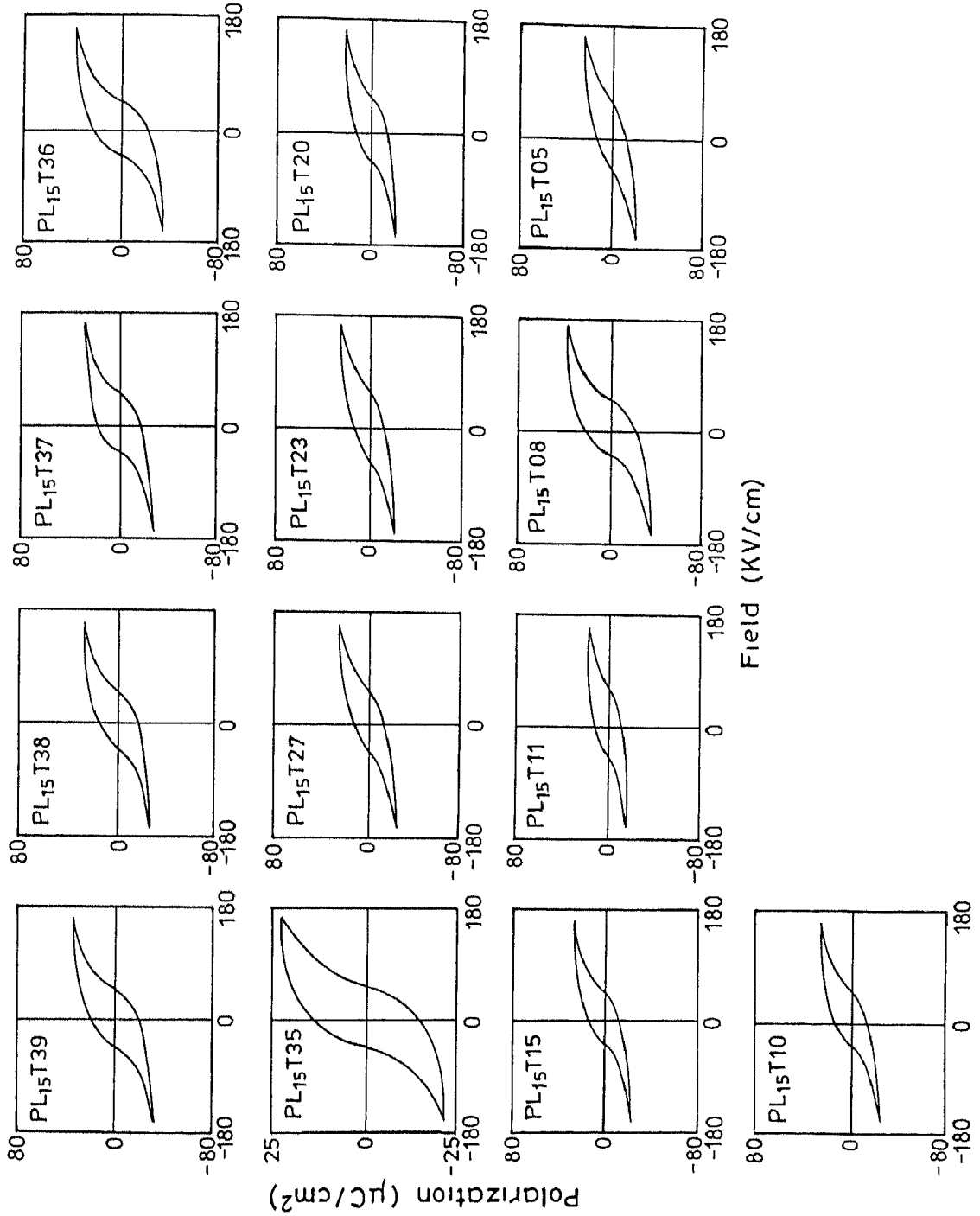

Figure 3 10 Hysteresis loops for the different devices on $PL_{15}T$ films the last two digits represent the number of the device

Table 3 10 Variation of P_s P_r and E_c values in $PL_{15}T$ film measured on different devices

Set No	Device Code	$P_s(\mu C/cm^2)$	Av P_s	$P_R(\mu C/cm^2)$	Av P_r	E_C(kV/cm)	Av E_c
	$PL_{15}T15$	22 5		12 5		55 0	
	$PL_{15}T20$	20 5		12 5		55 0	
	$PL_{15}T23$	22 5		14 5		55 0	
	$PL_{15}T27$	24 0		14 5		53 0	
I	$PL_{15}T35$	21 5	24 5	14 0	15 8	55 0	52 8
	$PL_{15}T36$	34 0		22 5		48 0	
	$PL_{15}T37$	24 0		16 0		52 0	
	$PL_{15}T38$	24 0		16 0		52 0	
	$PL_{15}T39$	28 0		20 0		50 0	
	$PL_{15}T05$	18 2		12 7		62 7	
	$PL_{15}T08$	23 8		13 6		54 5	
II	$PL_{15}T10$	35 0	24 4	22 5	15 1	46 5	52 3
	$PL_{15}T11$	21 3		13 1		51 7	
	$PL_{15}T15$	23 5		13 6		46 0	

Table 3 11 Variation of P_s P_r and E_c for the $PL_{15}T$ films reported in literature

Ref	Detail of the sample	P_S($\mu C/cm^2$)	P_R($\mu C/cm^2$)	E_C(kV / Cm)
[37] Schwartz et al	410 nm films prepared by Sol Gel method on $Pt/Ti/SiO_2/Si$ substrates Films were annealed at 600^0 C for 30 min	18 75	5 0	57 0
[10] Kang et al	~480 nm films were prepared by Sol Gel method on $Pt/Ti/SiO_2/Si$ substrates Films were annealed at 650^0 C for 30 min	6 67	2 67	31 7
[40] Nagao et al	150 nm thick films prepared by Rf sputtering method on (100) Pt and (100) MgO substrates	—	15 0	115 0
[36] Iijima et al	Films were prepared on (100) Pt substrate by rf sputtering method	46 0	36 0	35 5
[64] L Meidong et al	Films were prepared on several substrates by Sol Gel method	—	17 0	46 0

480 nm thick films are quite different from the values obtained by us (Table 3 10) for $PL_{15}T$ films This difference may be due to difference in thickness of the films substrate nature of the film or the difference in the heat treatment The P_s P_r and E_c values obtained from the paper of Iijima et al [36] also differ from our observed data (Table 3 10) but they used MgO single crystal and epitaxial Pt substrates for the film preparation and had the better C axis orientation $\alpha = 0\ 67$

The value of E_c (Table 3 10) obtained by us is almost twice the value obtained by Kang et al [10] and Iijima et al [36] which indicates the presence of stress in the films It is known that high stress may develop in sol gel deposited films

Fig 3 11 Fig 3 12 and Fig 3 13 show the hysteresis loops of the $PL_{12}C_{03}T$ $PL_{10}C_{05}T$ and $PL_{08}C_{07}T$ films respectively P_s P_r and E_c values from these hysteresis loops are shown in Table 3 12, 3 13 and 3 14 respectively

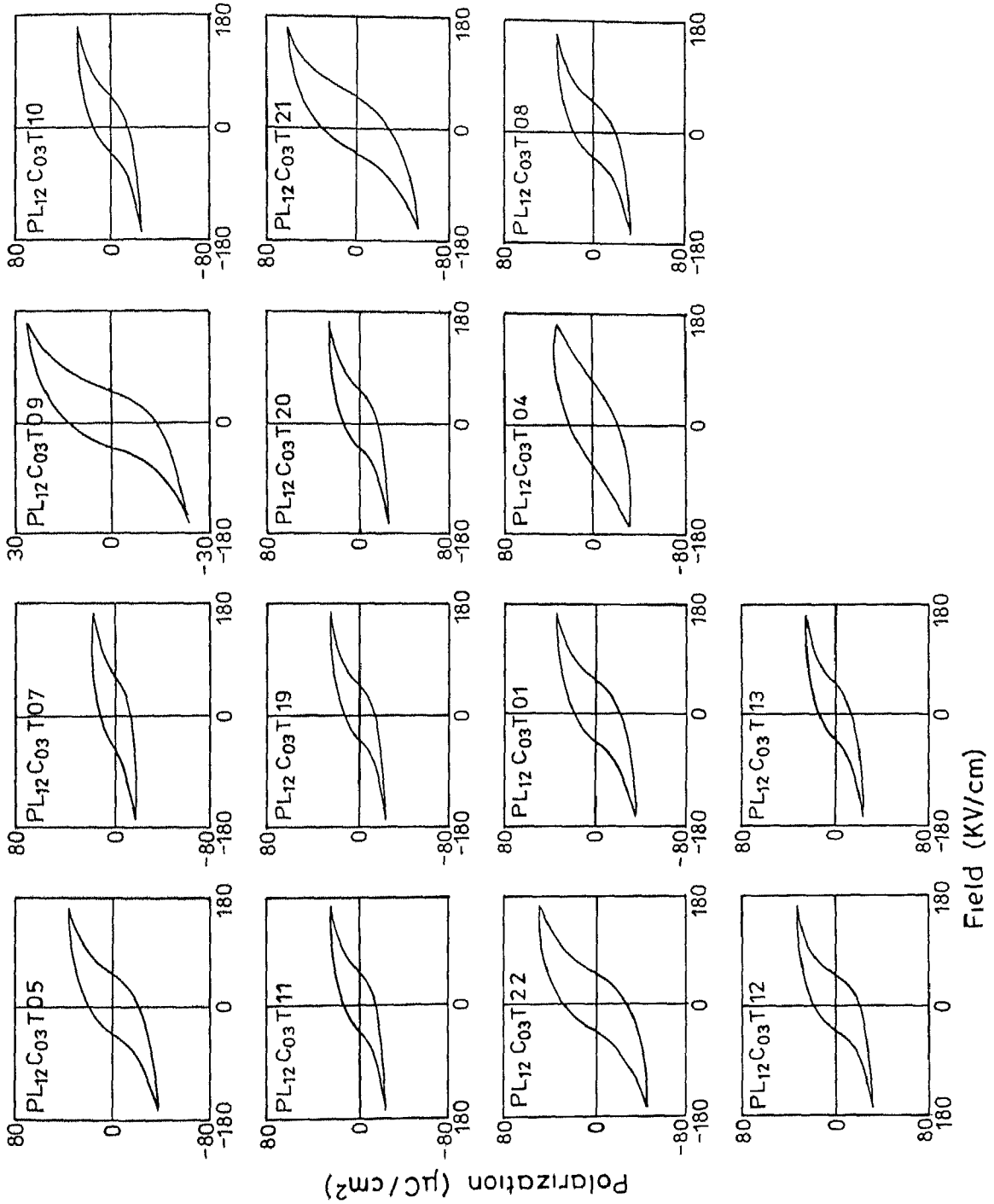

Figure 3 11 Hysteresis loops for the different devices on $PL_{12}C_{03}T$ films the last two digits represent the number of the device

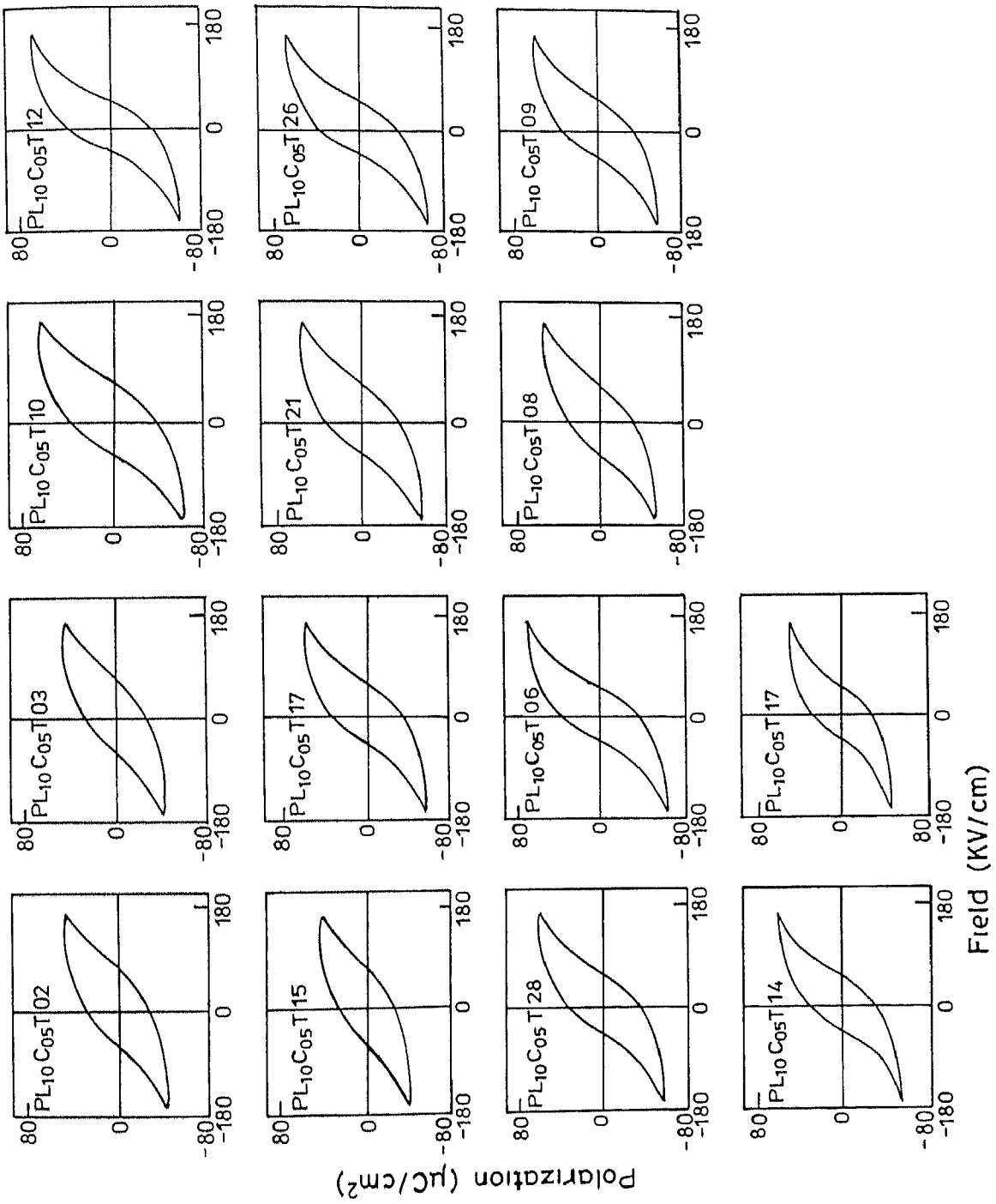

Figure 3 12 Hysteresis loops for the different devices on $PL_{10}C_{05}T$ films the last two digits represent the number of the device

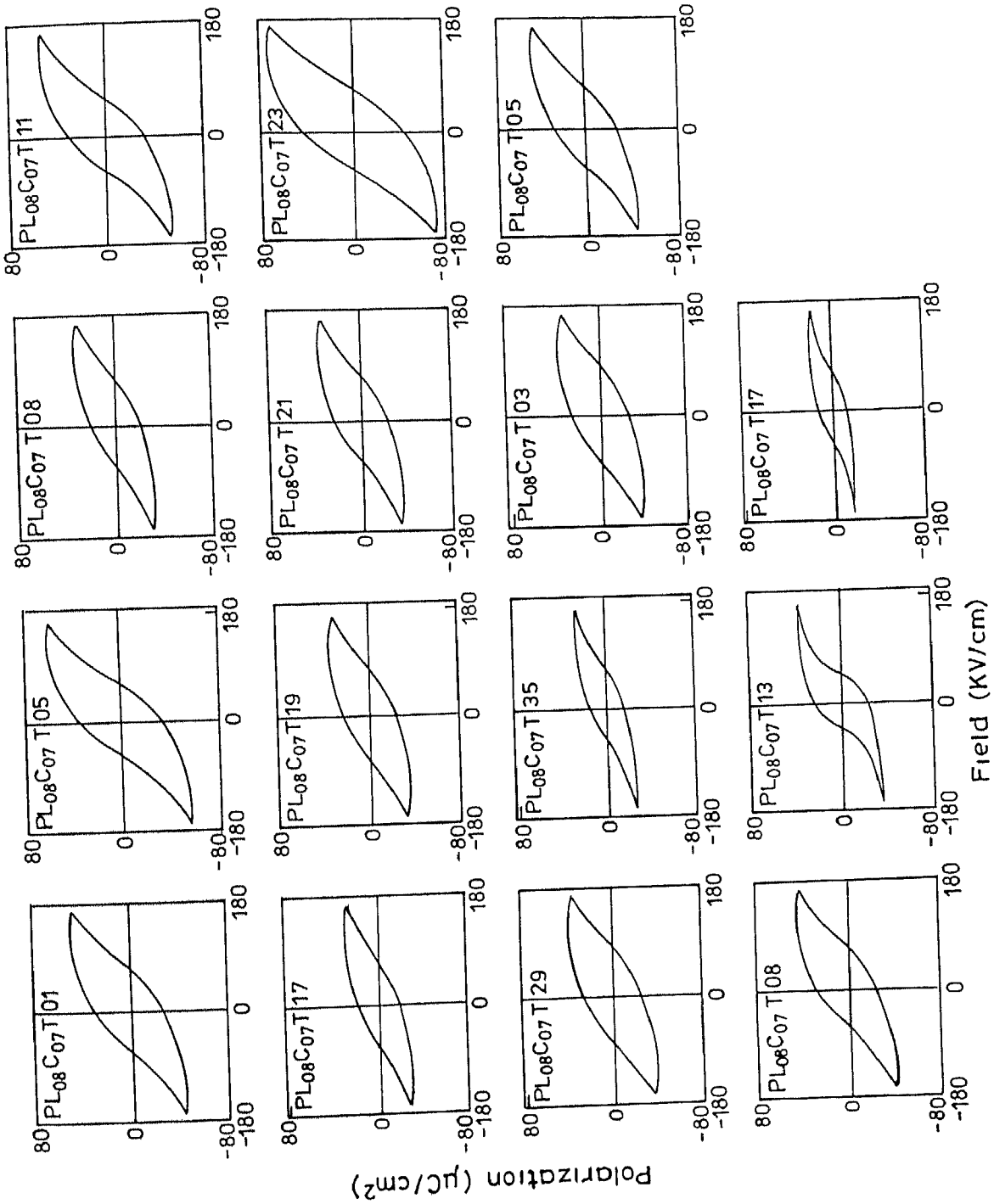

Figure 3 13 Hysteresis loops for the different devices on $PL_{08}C_{07}T$ films the last two digits represent the number of the device

Table 3.12 Variation of in P_s P_r and E_c in $PL_{12}C_{03}T$ films for different devices

Set No	Device Code	$P_s(\mu c/cm^2)$	Av P_s	$P_r(\mu c/cm^2)$	Av P_r	$E_c(kV/cm)$	Av E_c
	$PL_{12}C_{03}T05$	31 0		19 0		50 0	
	$PL_{12}C_{03}T07$	18 5		12 5		60 0	
	$PL_{12}C_{03}T09$	22 5		12 5		50 0	
	$PL_{12}C_{03}T10$	22 5		14 0		48 0	
I	$PL_{12}C_{03}T11$	21 0	28 6	14 0	17 8	50 0	50 5
	$PL_{12}C_{03}T19$	20 0		14 0		45 0	
	$PL_{12}C_{03}T20$	22 0		14 0		52 0	
	$PL_{12}C_{03}T21$	52 0		32 0		50 0	
	$PL_{12}C_{03}T22$	48 0		29 0		50 0	
	$PL_{12}C_{03}T01$	32 0		18 0		54 0	
	$PL_{12}C_{03}T04$	34 0		22 0		63 0	
II	$PL_{12}C_{03}T08$	22 0	28 3	19 0	18 4	49 0	53 0
	$PL_{12}C_{03}T12$	30 0		19 0		51 0	
	$PL_{12}C_{03}T13$	23 5		13 5		49 0	

Table3 13 Variation in P_s P_r and E_c in $PL_{10}C_{05}T$ films for different devices

Set No	Device Code	$P_s(\mu c/cm^2)$	Av P_s	$P_r(\mu c/cm^2)$	Av P_r	Ec(kv/cm)	Av E_c
I	$PL_{10}C_{05}T02$	45 0	54 9	28 0	33 8	67 5	58 4
	$PL_{10}C_{05}T03$	46 0		28 0		64 0	
	$PL_{10}C_{05}T10$	66 0		38 0		60 0	
	$PL_{10}C_{05}T12$	66 0		38 0		45 0	
	$PL_{10}C_{05}T15$	43 0		28 0		65 0	
	$PL_{10}C_{05}T17$	55 0		35 0		59 0	
	$PL_{10}C_{05}T21$	55 0		36 0		63 0	
	$PL_{10}C_{05}T26$	66 0		38 0		50 0	
	$PL_{10}C_{05}T28$	52 0		35 0		52 0	
II	$PL_{10}C_{05}T06$	62 0	58 3	36 5	36 7	52 0	51 0
	$PL_{10}C_{05}T08$	64 0		44 0		57 0	
	$PL_{10}C_{05}T09$	55 0		36 0		54 0	
	$PL_{10}C_{05}T14$	49 0		30 0		49 0	
	$PL_{10}C_{05}T17$	61 0		37 0		43 0	

Table 3 14 Variation in P_s, P_r and E_c in $PL_{08}C_{07}T$ films for different devices in

Set No	Device Code	$P_s(\mu c/cm^2)$	Av P_s	$P_r(\mu c/cm^2)$	Av P_r	$E_c(kV/cm)$	Av E_c
I	$PL_{08}C_{07}T01$	46 0	43 0	30 0	27 6	65 0	68 6
	$PL_{08}C_{07}T05$	60 0		34 0		60 0	
	$PL_{08}C_{07}T08$	34 0		22 0		65 0	
	$PL_{08}C_{07}T11$	52 0		34 0		58 0	
	$PL_{08}C_{07}T17$	30 0		18 0		65 0	
	$PL_{08}C_{07}T19$	34 0		24 0		80 0	
	$PL_{08}C_{07}T21$	35 0		25 0		72 0	
	$PL_{08}C_{07}T23$	75 0		46 0		72 0	
	$PL_{08}C_{07}T29$	40 0		28 0		83 0	
	$PL_{08}C_{07}T35$	25 0		15 0		66 0	
II	$PL_{08}C_{07}T03$	40 0	36 2	26 0	22 3	73 0	62 4
	$PL_{08}C_{07}T05$	48 0		27 0		70 0	
	$PL_{08}C_{07}T08$	43 0		25 5		68 0	
	$PL_{08}C_{07}T13$	32 0		21 0		50 0	
	$PL_{08}C_{07}T17$	18 0		12 0		61 0	

Fig 3 14 and 3 15 shows the variation of P_s P_r and E_c with change in Ce at % in the films respectively As the La/Ce ratio decreases P_s and P_r values increase first but after 5 at % of Ce, they decrease As the c axis is the polarization axis enhanced ferroelectric properties can be expected with the high value of c axis orientation in the films Earlier

Table 3 14 Variation in P_s P_r and E_c in $PL_{08}C_{07}T$ films for different devices in

Set No	Device Code	$P_s(\mu c/cm^2)$	Av P_s	$P_r(\mu c/cm^2)$	Av P_r	$E_c(kV/cm)$	Av E
I	$PL_{08}C_{07}101$	46 0	43 0	30 0	27 6	65 0	68 6
	$PI_{08}C_{07}105$	60 0		34 0		60 0	
	$PL_{08}C_{07}108$	34 0		22 0		65 0	
	$PL_{08}C_{07}T11$	52 0		34 0		58 0	
	$PL_{08}C_{07}T17$	30 0		18 0		65 0	
	$PI_{08}C_{07}119$	34 0		24 0		80 0	
	$PI_{08}C_{07}121$	35 0		25 0		72 0	
	$PI_{08}C_{07}123$	75 0		46 0		72 0	
	$PL_{08}C_{07}T29$	40 0		28 0		83 0	
	$PI_{08}C_{07}T35$	25 0		15 0		66 0	
II	$PL_{08}C_{07}T03$	40 0	36 2	26 0	22 3	73 0	62 4
	$PL_{08}C_{07}T05$	48 0		27 0		70 0	
	$PL_{08}C_{07}T08$	43 0		25 5		68 0	
	$PI_{08}C_{07}T13$	32 0		21 0		50 0	
	$PI_{08}C_{07}T17$	18 0		12 0		61 0	

Fig 3 14 and 3 15 shows the variation of P_s P_r and E_c with change in Ce at % in the films respectively As the La/Ce ratio decreases P_s and P_r values increase first but after 5 at % of Ce, they decrease As the c axis is the polarization axis enhanced ferroelectric properties can be expected with the high value of c axis orientation in the films Earlier

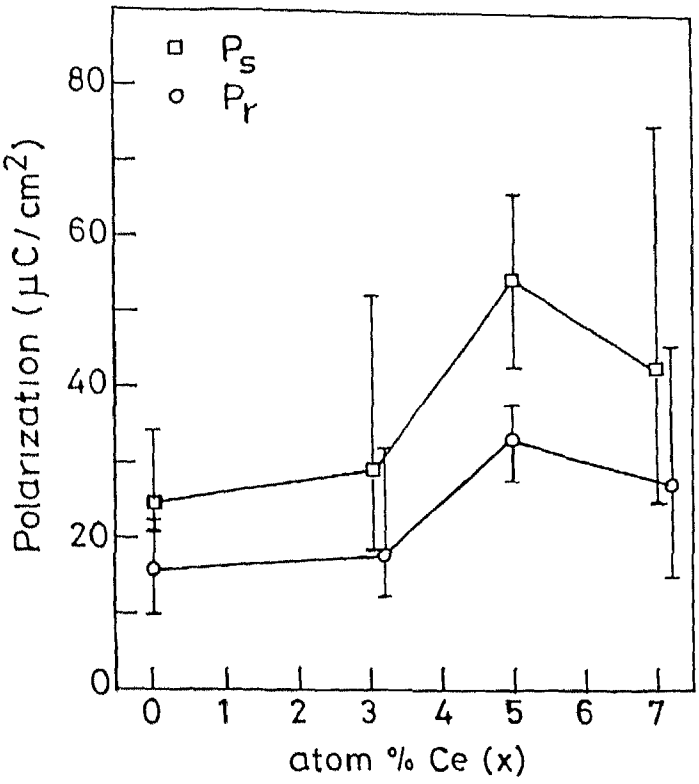

Fig 3.14 Variation of P_s and P_r with atom % Ce

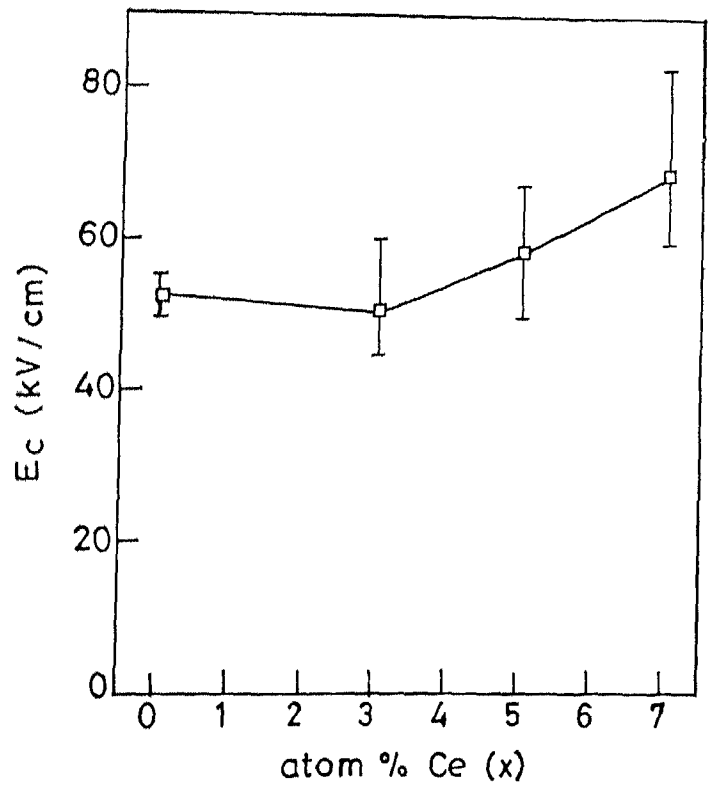

Figure 3.15 Variation of E_c with atom % Ce

while discussing the results of phase study by X ray diffraction in section 3 1 1 we had seen that the c axis orientation in our film is maximum for 5 at % Ce films (Fig 3 4) Thus the high value of the P_s and P_r at this composition can be attributed to increased C axis orientation in the film

According to Table 2 1 radius of Ce^{+3} and Ce^{+4} both are within 15% (Goldschmidt rule) of the radious of La^{+3} So there is a high chance for Ce to go to the A site in PLT films and substitute for La As the donor dopants increase the domain wall mobility and enhance the dielectric and ferroelectric properties [66] it can be concluded that relative occupancy of Ce at A site increase upto 5 at % of Ce After on further addition of Ce most probably it starts to precipitate a separate phase Majumder [61] worked on Ce doped PZT thin film system and showed that the values of P_s and P_r increase up to 1 atom % Ce and decrease for Ce> 1 atom % Although CeO_2 had not been detected by X ray or SEM below 10 % Ce Majumder concluded that Ce precipitated CeO_2 above 1 mole % of Ce doping and so decreased the hysteresis loop properties This is consistent with our case also Most probably in films with Ce > 5 atom % precipitation of CeO_2 occur and decreases the hysteresis loop characteristics due to pinning effect of the domain wall i e mobility of the domain wall decreases

Variation of E_c values with the amount of Ce in PLCT thin films is quite consistent with the above discussion Although it is hard to explain the slight increase of the values of E_c for $PL_{12}C_{03}T$ film from $PL_{15}T$ thin film the decreasing trend of E_c upto $PL_{12}C_{03}T$ and then its sudden increase is quite logical

3 4 2 Simulation of hysteresis loop

Polarization curve is related with the entire circuit rather than only the ferroelectric capacitor Variation in the process parameters and techniques may also influence the nature of the curves Ferroelectric materials have wide variety of physical features Miller et al [67] developed a physical model to separate the actual ferroelectric effects from other effects They have developed a model to simulate this behavior of a device and extract the material parameters Their physical model is shown in Fig 3 16 It consists of a ferroelectric capacitor circuit element containing a switchable ferroelectric layer of thickness d_f between two non switchable dielectric layers one each adjacent to the electrodes

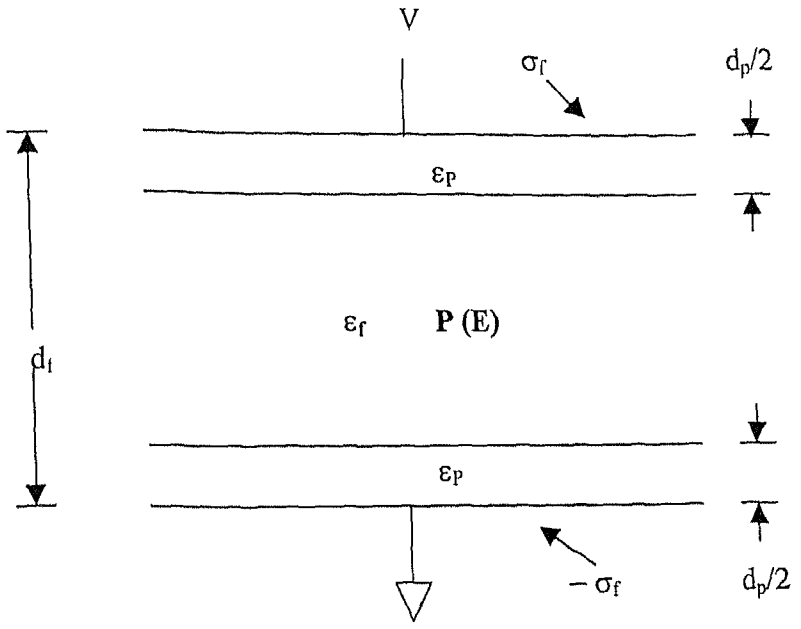

Fig 3 16 Physical model for hysteresis loop simulation [67]

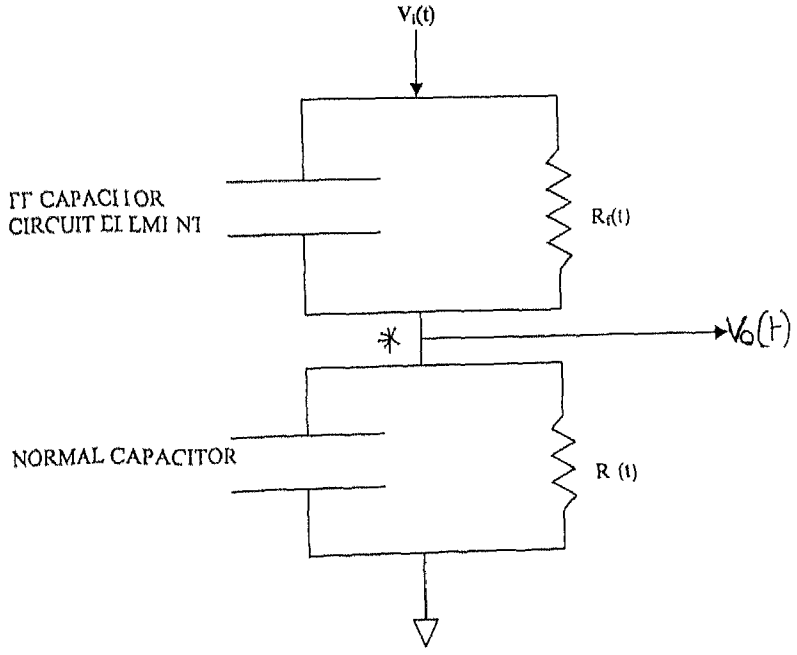

Fig 3 17 Modified Sawyer Tower circuit with parasite resistance used for simulation of the hysteresis loop[67]

Fig 3 17 shows the modified Sawyer Tower circuit used in this physical model Appendix B describes that physical model

In Fig 3 17 the following notifications are used

$V_i(t)$ = Voltage input

$V_0(T)$ = Voltage output across the standard capacitor

C_n = Capacitance of standard capacitors

R_f = Resistance of ferroelectric layer

R_n = Resistance of standard capacitor

d_p = Dielectric layer thickness

To determine the simulated hysteresis loop we use a computer programme (appendix C) Here P_s P_r E_c and R_f are the variables among the all parameters A high value resistance of ferroelectric layer (R_f) have been assumed and the P_s P_r and E_c values from the experimental data are used to simulate the loop These values have been changed to get the best fit of simulated loop with the corresponding experimental loop Fig 3 27 shows the simulated and experimental loops for $PL_{15}T$ $PL_{12}C_{03}T$ $PL_{10}C_{05}T$ and $PL_{08}C_{07}T$ respectively Table 3 15 Shows the simulated and experimental parameters of the $PL_{15}T$ $PL_{12}C_{03}T$, $PL_{10}C_{05}T$ and $PL_{08}C_{07}T$ films respectively

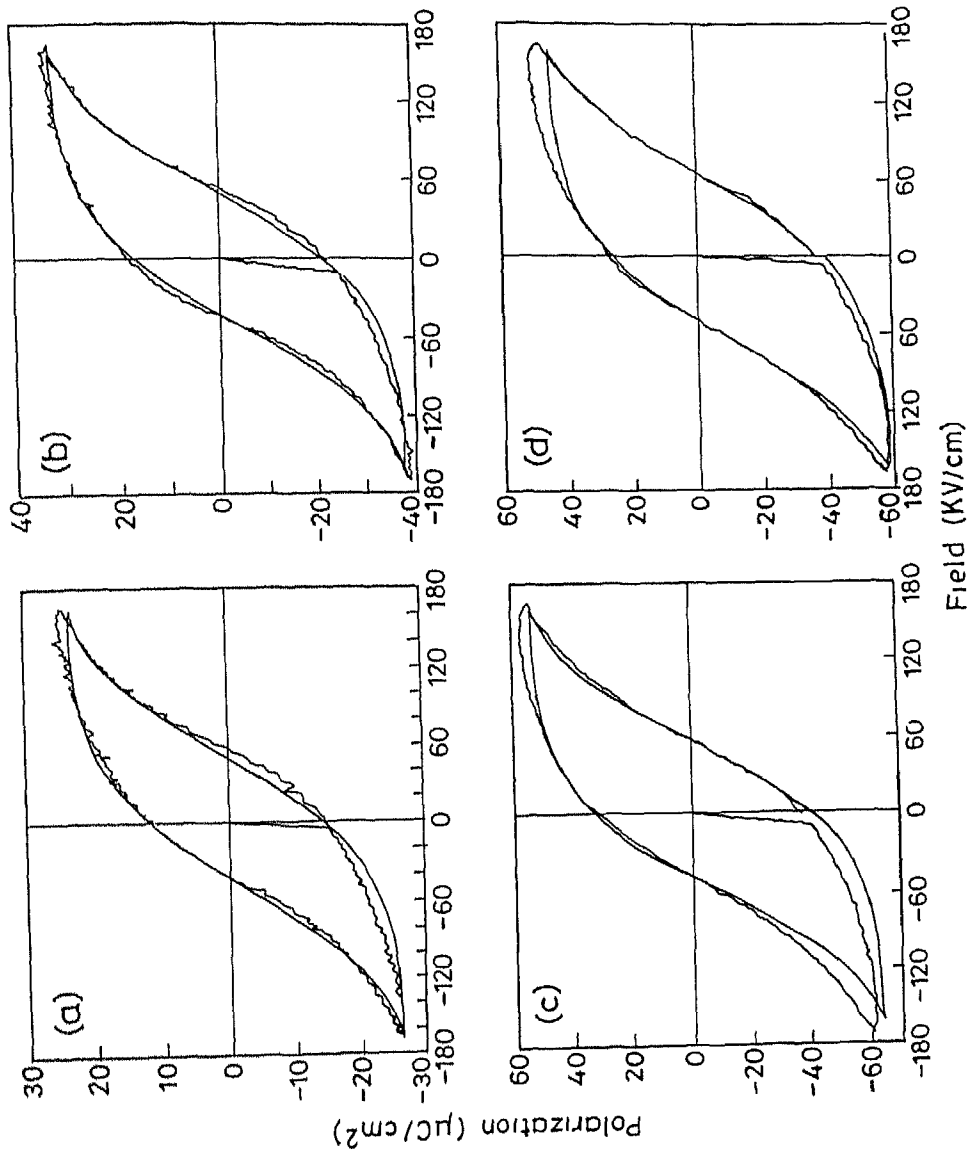

Fig 3 18 Simulated ( ) and experimental (~) hysteresis loops of the films (a) $PL_{15}T$ (b) $PL_{12}C_{03}T$, (c) $PL_{10}C_{05}T$ and (d) $PL_{08}C_{07}T$ respectively

Table 3 15 Variation of simulated and experimental hysteresis loops

Thin Film	$D_f(A^0)$	$R_f(A^0)$	$P_s(\mu c/cm^2)$	$P_r(\mu c/cm^2)$	E_c
$PL_{15}T$ (Sim)	0 00	10^{13}	26 5	14 0	48 46
$PL_{15}T$ (Exp)	—	—	23 1	13 0	48 46
$PL_{12}C_{03}T$ (Sim)	0 00	10^{13}	40 0	20 0	48 5
$PL_{12}C_{03}T$ (Exp)	—	—	36 0	20 0	48 5
$PL_{10}C_{05}T$ (Sim)	0 00	10^{13}	63 5	37 0	54 0
$PL_{10}C_{05}T$ (Exp)	—	—	56 4	34 4	54 0
$PL_{08}C_{07}T$ (Sim)	0 00	10^{13}	57 5	36 3	63 0
$PL_{08}C_{07}T$ (Exp)	—	—	50 0	32 2	58 15

From this simulation some conclusions can be drawn

1 The values of P_s and P_r have to be changed to match the simulated curves with the experimental one although the E_c values remain same in almost all the cases

2 From Fig 3 27 it is clear that the hysteresis loop for the $PL_{12}C_{03}T$ simulates the best

3 Simulation supports the absence of non switchable dielectric layer

3 4 3 Dielectric Characterization

The dielectric properties of the thin films are characterized in terms of dielectric constant (ε_r) and loss factor (tan δ) These properties depend on the substrate electrode used temperature frequency of measuring signal etc Table 3 16 summarizes the data from literature on the dielectric properties of the PLT thin films of different thickness La content and heat treatment temperature

Table 3.16 Summarize data on dielectric properties of PLT from literature

Ref	Temperature (^{0} C)	La content (at %)	Thickness (nm)	ε_r	tanδ
[38]	700 800	18.0	440 660	641 665 759 818	013 055
[37]	600^0 C/min	15.0	410	388	04
[12]	—	15.0	—	457	07
[11]	—	5.0 10.0	680 670	630 870	—
[8]	—	16.0 20.0	300	583 1130	—
[43]	—	15	—	1070	—

Fig 3.28 and Fig 3.29 show the variation of dielectric constant(ε_r) and dielectric loss (tanδ) with frequency for $PL_{15}T$, $PL_{12}C_{03}T$, $PL_{10}C_{05}T$ and $PL_{08}C_{07}T$ films respectively Fig 3.30 and Fig 3.31 show the variation of average dielectric constant (ε_r) and dielectric loss (tanδ) with the variation of Ce in PLT thin films measured at 100 KHz Dielectric constant and dielectric loss values for the film $PL_{15}T$ film are consistent with the values obtained by Adachi et al [43] (1070) and Schwartzm et al [37] (~0.07) respectively The trend in the dielectric constant variation is similar to the trend in P_s and P_r (Fig 3.24) For $PL_{10}C_{05}T$ film the dielectric constant value is highest (~ 1520) and before and after this composition the dielectric constant values drops abruptly In case of the variation of dielectric loss this trend is opposite For $PL_{10}C_{05}T$ film the dielectric loss is minimum (~0.07) while before and after this composition the dielectric loss values increase suddenly In the discussion of the electrical properties (chapter 3.4.1) we have concluded that Ce upto 5 at % substituted

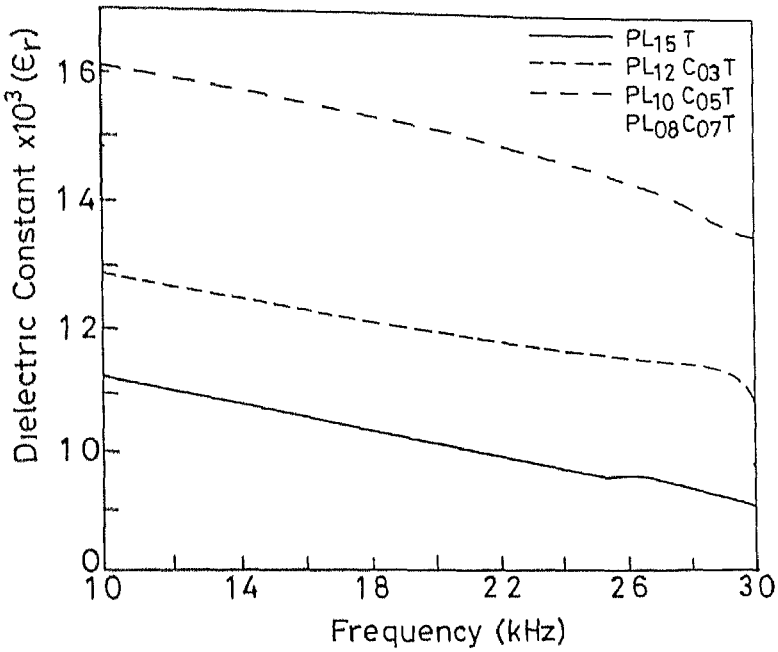

Fig 3 19 Variation of dielectric constant (ε_r) of the films with frequency

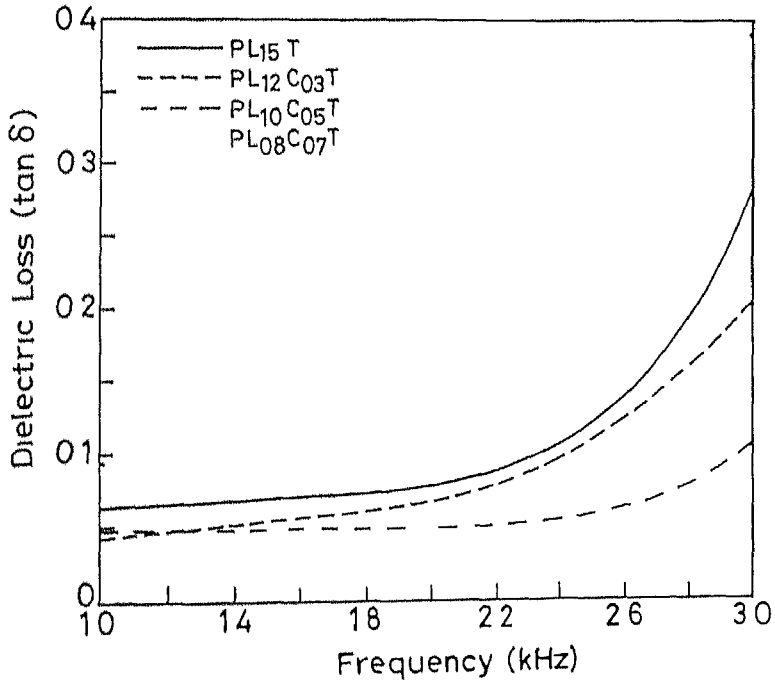

Fig 3 20 Variation of dielectric loss (tan δ) of the films with frequency

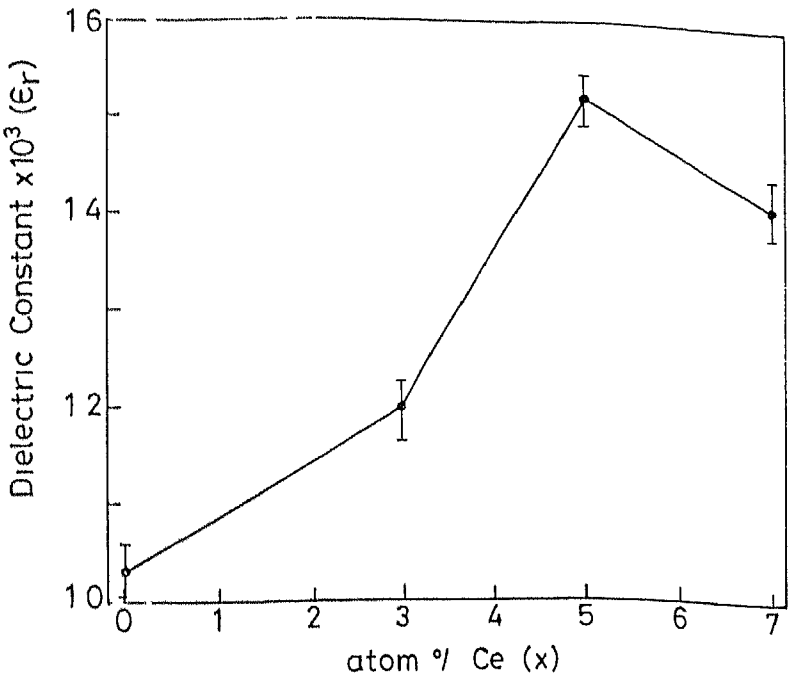

Figure 3.21 Variation of dielectric constant (ε_r) with atom % Ce

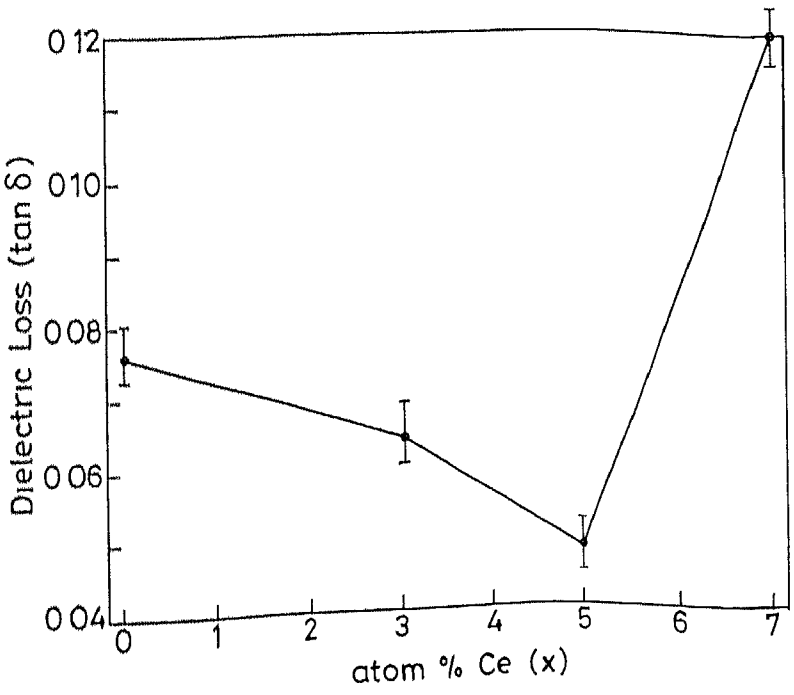

Figure 3.31 Variation of dielectric loss (tan δ) with atom % Ce

for La at A site of the perovskite PLT structure and acted as a donor Donor atoms increase the mobility of the domain walls This may be the cause for high P_s and P_r values in $Pb_{0.90}La_{0.10}TiO_3$ film That is known to increased domain mobility enhance the dielectric properties [65]

Chapter 4

Conclusion

In this work the effect of doping by Ce on the ferroelectric and dielectric properties of lead lanthanum titanate thin films has been studied For this study we chose the compositions of the films as $Pb_{0.9}La_{0.15-x}Ce_x[Ti_{0.9625}]O_3$ with x=0.0 0.03 0.05 and 0.07 respectively We prepared the films by sol gel method on polycrystalline Pt and single crystal sapphire substrates by spin coating method We studied the X ray diffraction of the films With increasing Ce content the C axis orientation of the films increases $I_{(001)}/I_0$ value is highest for the film with composition $PL_{10}C_{05}T$(~ >0.63) and decreases with further increase in Ce content The time temperature transformation (TTT) curve of the $PL_{15}T$ thin film shows that PLST crystallizes from amorphous to complete perovskite phase relatively at much lower temperature than in the PZT thin films Pyrochlore phase forms as an intermediate phase but it exists for a small time only Doping of Ce in the PLT thin films enhance its properties P_r P_s and ε_r values of the $P_{0.9}L_{0.15-x}Ce_xTi_{0.9625}O_3$ thin films increases upto 5 atom % Ce and decrease rapidly with further increase in Ce Saturation polarization remnant polarization and coercive field values of this film (PLCT with 5 atom % Ce) are 55 kV/cm^2 34 kV/cm^2 and 58 kV/cm respectively Ce is seem to be a donor dopant which substitutes for La from A site and enhances the easy of orientation of the domain wall in a field But above 5 at % Ce, excess Ce precipitates as CeO_2 and decreases the electrical properties by pinning the domains Variation of the electrical properties with the Ce content in the films is in agreement with the data obtained from $I_{(001)}/I_0$ vs atom % Ce curve With this investigation it has been seen that $PL_{10}C_{05}T$ has the best properties for the ferroelectric applications among the investigated thin films

References

[1] C B Sawyer and C H Tower Phys Rev **35** 269 (1930)

[2] G H Heartling Piezoelectric and electroptic ceramics in Ceramic materials for electronics edited by R C Buchanon Marcel Dekker Inc New York 139 (1986)

[3] M Okuyama and Y Hamakawa Preparation and basic properties of $PbTiO_3$ ferroelectric thin films Ferroelectrics **63** 243 (1985)

[4] K Iijima, Y Tomita, R Takayama and I Ueda Preparation of c axis oriented $PbTiO_3$ thin films and their crystallographic dielectric and pyroelectric properties J Appl Phys **60**(1), (1986)

[5] K Kushida and H Takeuchi, Epitaxial groth of $PbTiO_3$ films on $SrTiO_3$ by rf magnetron sputtering , IEEE Transactions on UFFC **38**(6) 656 62(1991)

[6] N Nagato, T Takeuchi and K Iijima Preparation and properties of (Pb La)TiO_3 pyroelectric thin films by rf magnetron sputtering Jap J Appl Phys **32**(part I 3B) 4065 68 (1993)

[7] D H Lee J S Lee, S M Cho H J Nan J H Lee J R Choi K Y Kim S T Kim and M Okuyama, 'Microstructure and electrical properties of (Pb La)TiO_3 thin films grown on the Pt electrodes with a percolating network structure Jap J Appl Phys **34**(I 5A) 2453 58 (1995)

[8] H Miwa and N Ichinose Dielectric properties of (Pb La)TiO_3 thin films by multiple cathode sputtering and its application to dynamic random access memory capacitors Jap J Appl Phys **35** (1 9B) 4976 79 (1996)

[9] K Tominaga M Miyajima Y Sakashita H Segawa and M Okada Preparation of c axis oriented PLT thin films by the metalorganic chemical vopour deposition method Jap J Appl Phys **29L**, 1874 76 (1990)

[10] S J Kang and Y S Yoon Optical and electrical properties of lanthanum modified lead titanate thin films with various lanthanum concentration Jpn J Appl Phys **36**(1 7A) 4459 65 (1997)

[11] K No, C G Choi D S Yoon T H Sung Y C Kim S Jeong and W J Lee Pyroelectric properties of sol gel derived lanthanum modified lead titanate thin films Jap J Appl Phys, **34**(1 5A), 2731 33 (1996)

[12] K K K Soc M Maeda and I Suzuki Sol gel processing of $Pb_{1-x}La_xTi_{1-x/4}O_3$ thin films' Jap J Appl Phys, **35** (1 1A) 205 9 (1996)

[13] Y M Kang, J K Ku and S Baik Crystallographic characterization of (Pb La)TiO_3 epitaxial thin films grown by pulsed laser deposition J Appl Phys **78**(4) 2601 6 (1995)

[14] K D Keefer in Better ceramics through chemistry eds C J Brinker D E Clerk and D R Ulrich (North Holand New York, 1984) 15 24

[15] L R Pohl and G D Osterholtz in Molecular Characterization of Composite Interfaces eds H Ishida and G Kumar (Plenum New York, 1985) 157

[16] L H Sommer and C G Frye, J Am Ceram Soc **82,** 3796 (1960)

[17] L H Sommer, C G Frey, M C Muslof, G A Parker, P G Rodewald K W Michael Y Okaya and P Pepinski, J Am Chem Soc, **83** 2210 (1961)

[18] L H Sommer G A Parker N C Lloyd C L Frey and K W Michael J Am Chem Soc **89,** 857 860 (1967)

[19] D R Uhlmann B J Zelinski and G E Wnek in Better ceramics through chemistry eds C J Brinker D E Clark and D R Ulrich (North Holand New York) 59 70 (1984)

[20] R E Timms J Am Chem Soc A 1969 1974 (1971)

[21] W G Klemperer V V Mainz and D M Miller A molecular building block approach to the synthesis of ceramic materials in Better ceramics through chemistry II eds C J Brinker D E Clark and D R Ulrich (Mat Res Soc Pittsburgh) 03 13 (1986)

[22] R K Iler The chymistry of silica (Wiley New York) 1979

[23] L C Klein Ann Rev Mater Sc **15** 227 48 (1985)

[24] B K Coltrin S M Melpolder and J M Salva Procedings of the IVth international conference on ultrastructure processing of ceramics glass and composites Feb 1989 Tucson AZ eds D R Uhlmann and D R Ulrich (Wiely New York)

[25] I Artaka T W Zerda and J Jones J Non crystalline Solids **81** 381 (1986)

[26] H Tsuchida Science of Polymers (Baihukan Tokyo) 85 (1985)

[27] S Sakka and K Kamaya J Non crystalline Solid **48** 31 48 (1982)

[28] L C Klein and G T Garvey Soluble silicates ACS Symp Series No 194 ed J S Falcone J Am Chem Soc Washington D C 293 (1982)

[29] V G Gavrilyachenko R I Spinko M A Martynenko and E G Fesenko Spontaneous polarization and coercive field of lead titanate , Sov Phys Solid State **121** 1203 (1970)

[30] V Bondaıenko V Gavrılyachenko E Levıt V Ultın and V Chkalova Effectıve pıezoelectrıc transducers on the basc of lead tıtanate crystal Scıentıfic Rep Unıv Lıthıanıan SSR Uıtıasonıc **9** 105 107 (1977)

[31] S Matsukara N Shokata and M Mıkamı Epıtaxıal growth of $PbTıO_3$ on $MgAl_2O_4/Sı$ substrates ın pıoc 5th ınt Meetıng ferroelectrıc materıals and theır appl Kyoto 1985 and Jap J Appl Phys 24 suppl **24** 3 10 12 (1985)

[32] M Okuyama T Ueda and Y Hamakawa Preparatıon of orıented $PbTıO_3$ ferroelectrıc thın fılms on sılıcon Jap J Appl Phys **24** Suppl 22 619 21 (1985)

[33] K Kushıda and H Takeuchı Solıd Phase epıtaxy of $PbTıO_3$ sıngle crystal Jpn J Appl Phys **24** Suppl 24 2 407 9 (1985)

[34] K Keızer G H Lansınk and A J Burggraaf Anomolous dıelectrıc behavıour of La(III) substıtuted lead tıtanate ceramıcs J Phys Chem Solıds **39** 59 63 (1978)

[35] K Keızer and A J Berggraaf Graın sıze effect on the ferroelectrıc pyroelectrıc transıtıon the dıelectrıc constant, and the lattıce parameters ın lanthanum substıtuted lead tıtanate Phys Status Solıdı A 561 69 (1974)

[36] K Lıjıma R Takayama Y Tomıta and I Ueda Epıtaxıal growth and the crystallograthıc dıelectrıc and pyroelectrıc propertıes of lanthanum modıfied lead tıtanate thın fılms J Appl Phys **60**(8) 2914 19 (1986)

[37] R W Schwartz B A Tuttle D H Doughty C E Land D C Goonow C L Hernandez T J Land and S F Mertınaze Preparatıon and characterızatıon of chemıcally derıved (Pb La)$TıO_3$ thın fılms IEEE tracsactıons on UFFC **38**(6) 677 83(1991)

[38] Y Shyımızu K H Udaykumar and L E Cross Preparatıon and electrıcal propertıes of lanthanum doped lead tıtanate thın fılms by sol gel method J Am Ceram S oc **74**((12) 3023 27 (1991)

[39] G R Fox and S B Krupanidhi Nonlinear electrical properties of lead lanthanum titanate thin films deposited by multi ion beam reactive sputtering J Appl Phys **74**(3) 1949 59 (1993)

[40] Ref 6

[41] H Maiwa N Ieinose and K Okazaki Fatigue and refreshment of (Pb La)TiO_3 thin films by multiple cathod sputtering Jap J Appl Phys **33** 5240 43 (1994)

[42] H Maiwa N Ichinose and K Okazaka Electrical properties of (Pb La)TiO_3 thin films fabricated by multiple cathod sputtering Jap J Appl Phys **33** (part I II) 6227 34 (1994)

[43] M Adachi M Kgai and A Kawabato Preparation and properties of [111] oriented PLT films by rf magnetron sputtering Procedings of SPIE The international society for applications 364 457 62 (1994)

[44] K Komaki T Kamada S Hayashi M Kilagawa R Takayama and T Hirao Preparation of pyroelectric $Pb_{1-x}La_xTi_{1-x/4}O_3$ thin films from ceramic target by rf-magnetron sputtering , Jap J Appl Phys **33**(2 3B) L443 46 (1994)

[45] K Takeshi K Kazubi H Shigenori K Masatoshi F Royoichi D Takashi and H Takashi Preparation of La modified lead titanate thin films by rf magnetron sputtering method nd their pyroelectric properties Jap J Appl Phys L **34**(2B) 233 235 (1995)

[46] H Maiwa N Ichinose and K Okazaki Crystallization structure of $PbTiO_3$ thin films by multiple cathod sputtering Jpn J Appl Phys **31** 3029 32 (1992)

[47] S S Lee and H G Kim Phase formation and ferroelectric properties of PLT thin films by MOCVD Int Ferroelectrics, **12**(2 4) 83-92 (1996)

[48] A Grill R Laibowitz D Beach D Neumayer and P R Duncombe Effect of base electrode on the crystallization and electrical properties of PLT Int ferro **14**(1 4) 211 17 (1997)

[49] T Ryoichi K Takashi H Shigenori F Satoru O Atsushi O Takashi and H Takashi Pyroelectric properties of La modified $PbTiO_3$ thin films and their applications Ferroelectrics **195** (1 4) 311 316 (1997)

[50] W Wensheng C Zhiming A Masatoshi and K Akira Preparation of Zr rich PZT and La doped $PbTiO_3$ thin films by rf magnetron sputtering and their properties for pyroelectric applications Int Ferro **12**(2 4) 251 61 (1996)

[51] H Maiwa C Nobomu and K Okuzaki Ferroelectric properties of (Pb La)TiO_3 films by multiple cathod sputtering IEEE international symposium on application of ferroelectricsds 1994 IEEE iscataway NJ USA 94CH3416 5 476 79

[52] K Iijima T Takeuchi N Nagao R Tokayama and I Ueda Preparation and properties of lanthanum modified $PbTiO_3$ thin films by rf magnetron sputtering IEEE international symposium on applications of ferroelectrics 53 58 (1994)

[53] S B Majumder Y N Mohapatra and D C Agrawal Fatigue resistance in lead zirconate titanate thin ferroelectric films effect of cerium doping and frequency Appl Phys Letter, **70** 138 (1997)

[54] S Chandra Superionic Solida North Holland publication 9 12 (1981)

[55] G Yi A Wu and M Sayer Preparation of Pb(Zr Ti)O_3 thin films by sol gel processing electrical optical and electro opticproperties J Appl Phys **64** 2717 (1988)

[56] L Pardo M Alguero and M L Calzade Microstructures and properties of La modified lead titanate sol gel processed thin films Ferroelectric Thin Films Proc COST 514 European Concerted Action Workshop F Leccabue B E Watts and G Bocelli eds Edizioni Ets Pisa Italy 82 85 (1997)

[57] R A Lipeles D J Coleman and M S Leung Effects of hydrolysis on metallo organic solution deposition of PZT films in better ceramics through chemistry II eds C J Brinker D E Clark and D R Ulrich **73** 645 (1986)

[58] C Kwak S B desu and D P Vijay Ferroelectric Letters **116** 143 (1994)

[59] C J Brinker and G W Scherer Sol Gel Science Academic Press New York (1990)

[60] J Zarrycki M Prossas and J Phalippau J Mater Sc **17** 3371 79 (1982)

[61] G Yi and M Sayer Sol Gel processing of complex oxide films Ceram Bull **70** 1173 (1991)

[62] S B Majumder Ph D Thesis Materials Science Programme IIT/Kanpur 1997

[63] B D Cullity, Elements of X Ray diffraction Addison Wesley Publishing Company Inc 324 333 (1967)

[64] Ref 60

[65] M Liu H Enpei WE Peiying R Yunhua Z Yike and L Chwang Preparation and properties of lead based ferroelectric thin films Mat Sc and Engg C Bio Materials Semcors and Systems **3** (3 4) 241 44 (19

[66] B Jaffe W R cook and M Jaffe Piezoelectric Ceramics Academic Press London (1971)

[67] S J Miller R D Schwank M S Rodgers and P V Dressedorfer Device modeling of ferroelectric capacitors J Appl Phys **64** (12) 6463 71 (1990)

Appendix A

Programming for the calculation of lattice parameters

```
#include<stdio h>
#include<math h>
#define lambda 1 54056
#define pi 3 1416
#define iteration 20

main()
{
float theta[50] h[50] k[50] l[50] a c c_a
float sum_x sum_xx sum_y sum_yy sum_z sum_zz sum_xy sum_xz t b g cs_sq
float m_a m_c c_y c_z p q a1 a2 b1 b2 d1 d2
int i=0 j=0 n=0
char ifile[10] ofile[10]
FILE *fpt  *spt
system( clear )
printf(               LATTICE PARAMETER CALCULATION FOR TETRAGONAL SYSTEM
 )
printf( \n\n\n\n\n\n\n\n )
printf(                              Enter Data File Name    )
scanf( %s  &ifile)
fpt = fopen(ifile  r )
  if(fpt == 0){
    printf( The File %s Does Not Exist In The Current
Directory\n\n\n  ifile)
    exit()
    }
sprintf(ofile  %s tet  ifile)
spt = fopen(ofile  w )
while(fscanf(fpt  %f %f %f %f  &theta[n] &h[n] &k[n] &l[n])!=EOF)
  {
    n++
  }
printf( \n       No  of Data=%d\n\n\n  n)
/*Initial c/a calculation*/
p=sin(pi/180*theta[0]/2)
q=sin(pi/180*theta[1]/2)
```

```
a1=l[0]*l[0]
a2=l[1]*l[1]
b1=p*p
b2=q*q
d1=(h[0]*h[0]+k[0]*k[0])
d2=(h[1]*h[1]+k[1]*k[1])
c_a=sqrt((a2*b1-a1*b2)/(d1*b2-d2 b1))

fprintf(spt  LATTICE PARAMETER CALCULATION OF TETRAGONAL SYSTEM FOR THE
INPUT FILE \ %s\ \n\n  ifile)
printf( Initial value of c/a =  f\n\n  c_a)
fprintf(spt  Initial value of c/a =  f\n\n  c_a)

for(j=0 j<iteration j++)
  {
    sum_x=0
    sum_xx=0
    sum_y=0
    sum_yy=0
    sum_z=0
    sum_zz=0
    sum_xz=0
    sum_xy=0
    fprintf(spt  Iteration No %d\n\n  (j+1))
    printf( Iteration No %d\n  (j+1))
    fprintf(spt  2(theta)        Cos^2(theta)        a                c\n )

   for(i=0 i<=n-1 i++)
       {
          t=(pi/180)*(theta[i]/2)
        b=lambda/(2*sin(t))
        g=(h[i]*h[i]+k[i]*k[i])
        a=b*sqrt(g+(l[i]*l[i])/(c_a*c_a))
        c=b*sqrt(g*(c_a*c_a)+(l[i]*l[i]))
          cs_sq=cos(t)*cos(t)
        sum_x=sum_x+cs_sq
        sum_xx=sum_xx+cs_sq*cs_sq
        sum_y=sum_y+a
        sum_yy=sum_yy+a*a
        sum_z=sum_z+c
        sum_zz=sum_zz+c*c
        sum_xy=sum_xy+cs_sq*a
        sum_xz=sum_xz+cs_sq*c
        fprintf(spt  \n%5 5f %15 5f %15 5f %15 5f  theta[i] cs_sq a c)
       }
    m_a=(sum_xy-(sum_x*sum_y/(float)n))/(sum_xx-(sum_x*sum_x/(float)n))
    m_c=(sum_xz-(sum_x*sum_z/(float)n))/(sum_xx-(sum_x*sum_x/(float)n))
    c_y=(sum_y/n)-m_a*(sum_x/(float)n)
    c_z=(sum_z/n)-m_c*(sum_x/(float)n)
    c_a=c_z/c_y
    fprintf(spt  \n\n          a = %f  c = %f  c/a =
%f\n\n\n  c_y c_z c_a)
    printf( \n a = %f  c = %f  c/a = %f\n\n\n  c_y c_z c_a)
 }
 fclose(fpt)
 fclose(spt)
 printf( \n            Results Available In %s \n\n\n  ofile)
```

```
printf(                                    Thank You\n\n\n\n )

}
```

Appendix B

Physical model for hysteresis loop simulation

In the modified circuit of Sawyer Tower a time dependent input voltage $V_i(t)$ is applied and an output voltage $V_0(t)$ get That output voltage as a function of time can be determined from the following equation

$$\frac{dV_0}{dt} = \frac{\gamma_3 c_f \left[\frac{dV(t)}{dt}\right] + \left[\frac{V(t)}{R_f(t)}\right] - V_0(t)\left\{\left[\frac{1}{R(t)}\right] + \left[\frac{1}{R_f(t)}\right]\right\}}{C + \gamma_3 C_f} \qquad (A1)$$

where

$$\gamma_3 = \frac{1}{\gamma_2}\left(1 + \frac{1}{\varepsilon_0 \varepsilon_f}\frac{\delta P_d(E\,t)}{\delta E}\right)$$

$$\gamma_2 = 1 - \frac{d_p}{d_f}\left[1 - \frac{\varepsilon_f}{\varepsilon_p}\left(1 - \frac{1}{\varepsilon_0 \varepsilon_f}\frac{\delta P(E\,t)}{\delta E}\right)\right]$$

and

$$C_F = \left(\frac{\varepsilon_0 \varepsilon_f}{d_f}\right) A_f$$

A hyperbolic tangent function is chosen to describe the saturated polarization $P_d^+(E)$ due to its convenient mathematical properties that it is consistent with the experimental data

$$P_i(E) = P \tanh \frac{[E - E]}{2\delta}$$

where

$$\delta = E \left[\log \left(\frac{1 + \frac{P}{P}}{1 + \frac{P}{P}} \right) \right]^{-1}$$

A triangular voltage wave front (dV_i/d_T= constant) is used in this study

Now at some initial value of time the electric field is given by

$$E_f = \frac{1}{d_f \gamma_1} \left[V_i - V_0 - \frac{d_p P_d}{\varepsilon_0 \varepsilon_f} \right]$$

where

$$\gamma_1 = 1 - \frac{d_p}{d_f} \left(1 - \frac{\varepsilon_f}{\varepsilon_p} \right)$$

If field is known dP_d/dE can be calculated γ_3 and γ_2 can be computed by using this value and finally the value of dV_0/dt is calculated from the equation (A 1) Once the initial initial values of these necessary functions are determined the time is then incremented The output voltage at the T^h increment in time is given by

$$V_i = V_{i-1} + \frac{dV_0}{dt_{i-1}} (t_i - t_{i-1})$$

The value of the field at the T^h increment is given by

$$E_{fi} = \frac{V_i - V_i - \left(\frac{d_p}{\varepsilon_0 \varepsilon_f} \left[P_{d_{i-1}} - \left(\frac{dP_d}{dE_{i-1}} \right) E_{f_i} \right] \right)}{d_f \gamma_1 + \left(\frac{d_p}{\varepsilon_0 \varepsilon_f} \right) \left(\frac{dp_d}{dE_{i-1}} \right)}$$

and the dipole polarization is given by

$$P_{di} = P_{d_{i-1}} + \frac{dP_d}{dE_{i-1}} \left(E_{f_i} - E_{f_i} \right)$$

The l^{th} value of dP_d/dE is then calculated and finally l^{th} value of (dV_0/dt) is calculated The above procedure is applied repeatedly to determine the behaviour of the circuit as a function of time

Appendix C

Programming for the hysteresis loop simulation

```
*       IMPLICIT DOUBLE PRECISION (A-H O-Z)
*
        PARAMETER (DP =0 0  DF = 0 4E-4  EPSO = 8 854E-14
     +  EPSF = 600 0  EPSP = 1  CN - 10 OE-9  PR = 14 OE-6
     +  RF = 1 OE18  RN = 1 OE6  AREAF = 1E-4  PS = 23 OE-6
     +  EC = 45 OE3)
*
        COMMON /A1/ TIME
        COMMON /V1/ VPEAK TPERD4 SLOPE VDERI TPERD3
*
c        WRITE(* *) ENTER FREQUENCY AND PEAK OF TRIANGULAR INPUT
c        READ(* *)FREQ VPEAK
c        WRITE(* *) ENTER TIME STEP AND FINISH TIME
c        READ(* *)STEP FINTIM
        TPERIOD =1E-5
        NPOINTS = 100
        VPEAK=10
```

```
*
        STEP=TPERIOD/NPOINTS
        FINTIM=TPERIOD
*
        OPEN(23 FILE= 01 PRN )



*
        TIME = -STEP
        TPERD4 = TPERIOD/4 0
        TPERD3 = (3 0/4 0)*TPERIOD
        SLOPE = (VPEAK/TPERD4)
*



        GAMMA1 = 1 0 - (DP/DF)*(1 0 - (EPSF/EPSP))
* SETTING INITIAL CONDITIONS
        PDINIT = -PR
        VINIT =0 0
        VOINIT=  PDINIT*AREAF/CN
        EFINIT=(1 0/(DF*GAMMA1))*(VINIT-VOINIT- (DP*PDINIT)/(EPS0*EPSP))
        EF=  EFINIT
        PDF= PDINIT
        VOUT=VOINIT
*
100     TIME = TIME+STEP
        EFP=EF
        VOUTP=VOUT
        PDFP=PDF
        VINPUT = V(TIME)
*       WRITE(* *)  INPUT   TIME VINPUT VDERI
*
```

```
* CALCULATION OF OUTPUT VOLTAGE

*        GENERATION OF POLARISATION AND ITS DERIVATIVE

         IF (VDERI LT 0 0) THEN

          DPDF =DPD(-EF EC PR PS)

                              2

         ELSE

          DPDF = DPD(EF EC PR PS)

         ENDIF

         TEMPO1 = (EPSF/EPSP)*(1 0 + (1 0/(EPS0*EPSF))*DPDF)

         GAMMA2 = 1 0 - (DP/DF)*(1 0 - TEMPO1)

         TEMPO2 = (1 0 + (1 0/(EPS0*EPSF))*DPDF)

         GAMMA3 = (1 0*TEMPO2)/GAMMA2

         CF = (EPS0*EPSF*AREAF)/DF

*        WRITE(* *)  GAMMA   TIME GAMMA2 GAMMA3 CF

*

*                 CALCULATION OF RATE OF CHANGE OF OUTPUT VOLTAGE

         TEMPO3 = GAMMA3*CF*VDERI + (VINPUT/RF)

         TEMPO4 = VOUT*((1 0/RN)+(1 0/RF))

         DEVOUT = (TEMPO3-TEMPO4)/(CN+(GAMMA3*CF))

         VOUT = VOUTP +(DEVOUT*STEP)

*

*

* CALCULATION OF ELECTRIC FIELD (EF)

          TEMPO5 = PDF - (DPDF*EFP)
```

```
            TEMP06 = (DF*GAMMA1) + (DP/(EPS0*EPSP))*DPDF
            TEMP07 = VINPUT - VOUT - (DP/(EPS0*EPSP))*TEMP05
            EF = TEMP07/TEMP06
*           ----------------------------------------

            PDF = PDFP + DPDF*(EF - EFP)

*           ----------------------------------------
             WRITE(* *)  EF & PDF    TIME EF PDF
*           WRITE(* *)TIME EF PDF VDERI
*           WRITE(23 *)EF PDF
*           WRITE(* *)  DPDF    TIME DPDF
*
            WRITE(23 *)EF VOUT PDF VINPUT TIME
*101        format(4f20 8)
*
          IF (TIME LT FINTIM) GO TO 100
*
          STOP
          END

          REAL FUNCTION PD(EF EC PR PS)
          COMMON /A1/ TIME
          DEL = EC*((LOG10((1 0+PR/PS)/(1 0-PR/PS)))**(-1))
*         WRITE(* *)  DEL-PD    DEL EC PR PS
          PD = -PS*TANH((EF-EC)/(2 0*DEL))
          RETURN
          END
```

```
      REAL FUNCTION V(T)
      COMMON /V1/ VPEAK TPERD4 SLOPE VDERI TPERD3
       IF (T  LE  TPERD4) THEN
         V=SLOPE*T
         VDERI=SLOPE
       ELSEIF ( T LE TPERD3) THEN
```



```
         V=VPEAK-SLOPE*(T-TPERD4)
         VDERI=-SLOPE
       ELSE
         V=-VPEAK+SLOPE*(T-TPERD3)
         VDERI=SLOPE
       ENDIF
       RETURN
       END

      REAL FUNCTION DPD(EF EC PR PS)
      COMMON /A1/ TIME
      DEL = EC*((LOG((1 0+PR/PS)/(1 0-PR/PS)))**(-1))
*     WRITE(* *)  DEL-DPD   DEL EC PR PS
      PCOSH = (COSH((EF-EC)/(2 0*DEL)))**2
      DPD = PS*((2 0*DEL*PCOSH)**(-1))
      WRITE(24 *) DPD EF
      RETURN
      END
```